WILDFIRE SIMULATIONS FOR CALIFORNIA'S FOURTH CLIMATE CHANGE ASSESSMENT: PROJECTING CHANGES IN EXTREME WILDFIRE EVENTS WITH A WARMING CLIMATE

A Report for:

California's Fourth Climate Change Assessment

Prepared By:
Anthony Leroy Westerling, UC Merced

Edmund G. Brown, Jr., *Governor*

August2018
CCCA4-CEC-2018-014

ACKNOWLEDGEMENTS

This work was supported by the California Energy Commission, Agreement Number 500-14-005.

PREFACE

California's Climate Change Assessments provide a scientific foundation for understanding climate-related vulnerability at the local scale and informing resilience actions. These Assessments contribute to the advancement of science-based policies, plans, and programs to promote effective climate leadership in California. In 2006, California released its First Climate Change Assessment, which shed light on the impacts of climate change on specific sectors in California and was instrumental in supporting the passage of the landmark legislation Assembly Bill 32 (Núñez, Chapter 488, Statutes of 2006), California's Global Warming Solutions Act. The Second Assessment concluded that adaptation is a crucial complement to reducing greenhouse gas emissions (2009), given that some changes to the climate are ongoing and inevitable, motivating and informing California's first Climate Adaptation Strategy released the same year. In 2012, California's Third Climate Change Assessment made substantial progress in projecting local impacts of climate change, investigating consequences to human and natural systems, and exploring barriers to adaptation.

Under the leadership of Governor Edmund G. Brown, Jr., a trio of state agencies jointly managed and supported California's Fourth Climate Change Assessment: California's Natural Resources Agency (CNRA), the Governor's Office of Planning and Research (OPR), and the California Energy Commission (Energy Commission). The Climate Action Team Research Working Group, through which more than 20 state agencies coordinate climate-related research, served as the steering committee, providing input for a multisector call for proposals, participating in selection of research teams, and offering technical guidance throughout the process.

California's Fourth Climate Change Assessment (Fourth Assessment) advances actionable science that serves the growing needs of state and local-level decision-makers from a variety of sectors. It includes research to develop rigorous, comprehensive climate change scenarios at a scale suitable for illuminating regional vulnerabilities and localized adaptation strategies in California; datasets and tools that improve integration of observed and projected knowledge about climate change into decision-making; and recommendations and information to directly inform vulnerability assessments and adaptation strategies for California's energy sector, water resources and management, oceans and coasts, forests, wildfires, agriculture, biodiversity and habitat, and public health.

The Fourth Assessment includes 44 technical reports to advance the scientific foundation for understanding climate-related risks and resilience options, nine regional reports plus an oceans and coast report to outline climate risks and adaptation options, reports on tribal and indigenous issues as well as climate justice, and a comprehensive statewide summary report. All research contributing to the Fourth Assessment was peer-reviewed to ensure scientific rigor and relevance to practitioners and stakeholders.

For the full suite of Fourth Assessment research products, please visit climateassessment.ca.gov. This report contributes to energy sector resilience by providing wildfire scenarios that incorporate impacts of climate change.

ABSTRACT

Statistical models of large wildfire presence, number and size were developed for California and used to simulate individual large fire events under a wide range of future climate scenarios, as well as population and development footprint scenarios based on low, medium and high growth scenarios for the State; and three fuels treatment scenarios (0%, 50% and 90%) for Sierra Nevada forests. A large library of extreme fire events—consisting of more than 45 million statewide maps of large wildfires simulated monthly at 6 kilometer x 6 kilometer resolution for 1952-2099 for multiple statistical simulations for each combination of climate, population, development footprint and fuels management—was constructed to facilitate analyses of the impact of changes in extreme events on resources in the state. Mean annual area burned increased by 77% statewide under high (RCP 8.5) global greenhouse emissions pathways, while maximum area burned statewide increased by 178% by end of century. Extreme wildfire events increased in frequency, with fires greater than 10,000 hectares occurring nearly 50% more often. Simulated large-scale fuels treatments in Sierra Nevada forests substantially reduced increases in burned area, particularly in more moderate (i.e., mid-21st Century or lower cumulative global emissions) climate change scenarios.

Keywords: Wildfire, California, Climate Change, Drought, Tree Mortality, Extreme Events

Please use the following citation for this paper:

Westerling, Anthony Leroy. (University of California, Merced). 2018. ***Wildfire Simulations for California's Fourth Climate Change Assessment: Projecting Changes in Extreme Wildfire Events with a Warming Climate.*** California's Fourth Climate Change Assessment, California Energy Commission. Publication Number: CCCA4-CEC-2018-014.

HIGHLIGHTS

- This study contributes to the literature by moving beyond projections of changes in mean large fire occurrence, area burned, or fire danger, to create a resource for examining changes in the rare but impactful individual extreme fire events that account for most of the effects of fire on natural and human resources.
- As California's climate warms, the models used in this study indicate the greatest increases in burned area are projected to be in forested areas, with annual average area burned in many parts of the Sierra Nevada doubling to quadrupling by end of century (comparing 2070-2099 to 1961-1990) under the most extreme warming.
- Increasing burned area with warming temperatures, particularly in montane forests of the northern two thirds of the state, and a greater share of burned area coming from extremely large fires, is consistent with recent experience in California and around the arid western United States.
- Fuel treatments have the potential to substantially mitigate increases in burned area over much of the Sierra Nevada. A management scenario that treated about 30 percent of vegetated area reduced the increase in Sierra Nevada area burned by end of century by 16 - 31 percent (comparing 2070-2099 to 1961-1990).
- The impact of dead heavy fuels from tree mortality on wildfire after the first few decades, when heavy fuels have had time to cure and additional new biomass has developed, is without historical analogue for the scale of the recent dieback in the Sierra Nevada and cannot be quantified with empirical statistical models.
- Near-term impacts of tree mortality on severely burned acreage via the effects of the desiccation and subsequent movement of fine fuels from the forest canopy to the surface are expected to be small (1% to 7%) relative to natural system variability.
- The December 2017 Thomas fire in coastal southern California--the first wintertime megafire and briefly the largest fire in state history—occurred against a backdrop of factors that may become more common in the future. These include a very wet previous winter that increased fine fuel growth; an extreme, multiyear drought that left standing dead fuels; record warmth combined with no significant precipitation from Fall into December that helped to desiccate fuels; and an extended high wind event at the time of the fire. Ongoing efforts to understanding how these events may co-occur in the future will improve our assessment of the likelihood of future fire events of similar timing and magnitude and our ability to plan for more fire-safe communities.

TABLE OF CONTENTS

1: Introduction

A rapidly warming climate may increase wildfire in California and the western United States in the near term, particularly in montane forests of the region, as greater evapotranspiration combines with highly variable precipitation to produce more frequent and intense droughts with drier vegetation. This may already be occurring, as significant increases in burned area in recent decades have been associated with warmer temperatures and increased climate water deficit (Westerling et al 2006, Westerling 2016), and half or more of these increases have been attributed to anthropogenic warming effects on fuel aridity (Abatzoglou and Williams 2016).

Recent western US droughts of the 21st century—notably the California-centered drought beginning in 2012—were associated with an increased incidence of temperature and precipitation extremes compared to major 20th century droughts, and prolonged drought conditions westside have been associated with increased area burned and greater fire severity (Crockett and Westerling 2018).

Direct and indirect effects of warming are projected to significantly further increase forest wildfire in California, and western and Boreal forests more generally, by the mid-21st century (Kitzberger et al 2017). Similarly, western US forest area burned, fire danger, and smoke emissions are projected to increase in coming decades (Brown et al 2004, Spracklen et al 2009, National Research Council 2011, Hurteau et al 2014). Other studies for California specifically have projected significant increases in wildfire activity, particularly in forests (Fried et al 2004, Lenihan et al 2008, Westerling and Bryant 2008, Westerling et al 2011a, Batllori et al 2013).

Increased wildfire activity implies a range of direct and indirect impacts. Fire plays an important natural role in California's fire-adapted ecosystems, and average annual area burned in California was higher than present in some ecosystems prior to implementation of effective fire suppression in the 20th century. At the same time, the combination of a warming climate with accumulating fuels from fire suppression in forested areas is resulting in increased incidence of uncharacteristically severe fire with negative ecosystem impacts such as regrowth failure, habitat loss, reduced carbon storage, and reduced water quality (Stephens et al 2007, Miller et al 2009, Jones et al 2016, Liang et al 2014, Smith et al 2011), and changes to timing and quantity of runoff and recharge (Ffolliott et al 1989). While direct wildfire-induced deaths, injuries, and property losses can be significant, as was seen in the 2017 coastal northern and southern California wildfires, an even larger population is affected by wildfire air pollution induced morbidity, mortality, and lost productivity (Reese 2017, Kunzli et al 2006, Silva et al 2017, Fann et al 2018).

This study contributes to this literature by moving beyond projections of changes in mean large fire occurrence, area burned, or fire danger, to create a resource for examining changes in the rare but impactful individual extreme fire events that account for most of the effects of fire on natural and human resources. (While large fires are increasing in frequency, and the record for 1984 to 2013 contains more than 1300 large fires, there are still more than three and a half million monthly gridded time and location combinations with no large fires present (9922 grid cells x 30 years x 12 months = 3,571,920). The system of statistical models described here was used to create large libraries of simulated fire histories with repeated draws for future scenarios defined by global emissions pathways, climate model sensitivities to global greenhouse gas atmospheric concentrations, population growth, and development footprint. They were also

constructed so as to facilitate the incorporation of fuels management and drought-related dieback (see appendix B) scenarios on federal forests in the Sierra Nevada. By understanding how extreme wildfire events may change under different climate scenarios, stakeholders can begin to explore how climate change may impact resources in the state through wildfire.

Throughout this work, we use the term "extreme" fires to refer to statistically extreme events—the occurrence of some of the largest fires in the record—rather than to the impacts of those fires, which may be both positive and negative at the same time when assessed along different dimensions. For example, an extreme fire event could be at once net beneficial in its effects on habitat while at the same time exposing a large human population to harmful air pollution and imposing significant costs for management and for public and private built infrastructure. The next sections describe a system of three probability models conditional on climate and land surface characteristics, including a binomial model of large fire presence, a Poisson lognormal model for fire number, and generalized Pareto models for area burned in large fires. Together, these models describe a complex, compound distribution of area burned in extreme fire events in California conditional on climate, topography, population, and development footprint, and Sierra Nevada forest fuels management. An overview of model performance versus historical observations is then given, followed by examples drawn from future wildfire simulations. Appendix B extends this analysis to include scenarios for fire severity in response to forest mortality related to the recent, historically unprecedented severe drought centered on California.

2: Data and Methods

2.1 Data

2.1.1 Spatial and Temporal Domain

Fire activity is simulated over the state of California at a monthly time step from 1953 through 2099 on a 1/16-degree lat/long grid (~6 kilometer [km] resolution). Areas of the state outside the current combined fire state and federal protection responsibility areas have been excluded. This primarily excludes parts of the state landscape intensively converted to human uses—agricultural and urbanized areas—where large wildfires are uncommon and local fire protection is chiefly concerned with structure fires and small vegetation fires. Some additional areas of the state, primarily desert areas near the border with Mexico, are also excluded because population and vegetation scenarios excluded these areas. The fraction of each grid cell in combined federal and state fire protection responsibility area (*FSR*), as opposed to local protection responsibility, is also included as a potential explanatory value.

2.1.2 Fire History

Fire history data for large (>400 ha) wildfires were extracted from the Monitoring Trends in Burn Severity database (MTBS 2016, www.mtbs.gov; accessed 12/2008 and 9/2016), and coded by discovery date (month, year). We used ESRI Arc Macro Language (ESRI 1999) to intersect burn maps with a 1/16th degree grid, assigning each fire to the grid cell where a majority of area burned (Keyser and Westerling 2017). We then calculated total area burned as well as fractional area burned in six severity classes (unburned to low severity, low severity, moderate severity, high severity, increased greenness, or unclassified) by voxel (latitude, longitude, year ×

month) (Eidenshink et al 2007). MTBS data are comprehensive for fires >400 ha, based on remote imagery pre- and post-fire cross-tabulated with documentary fire records, and are available with the commencement of the satellite record in 1984. Statistical wildfire models were estimated using historical fire and climate data available for 1984–2013. These years encompass an historically broad range of climatic conditions, including the most extreme multiyear drought (2012-2015) in either the modern record or paleo-reconstructions for the last millennium and two of the three wettest years on record (2016-2017, 1997-1998), as well as a significant regional anthropogenic warming trend that has been detectable since the mid-1980s (Barnett et al 2008, Griffin and Anchukaitis 2014, Crockett and Westerling 2018, http://cdec.water.ca.gov/cgi-progs/products/PLOT_FSI.pdf).

2.1.3 Population, Vegetation, Ownership

Gridded population (*POP*) and vegetated fraction (VFR) were obtained from land use and land cover (*LULC*) and population scenarios for the state of California provided by Sleeter et al (2017) for the period 1970-2101. For the 1970-2001 period, scenarios use the USGS LUCAS model to "backcast" *LULC*, beginning with the 2001 initial conditions and ending with 1970. For future scenarios, the same model was initialized in 2001 and run forward on an annual time step to 2100. We obtained simulations with 10 Monte Carlo replications, including an historical backcast from 2001-1970 and three projections based on California Department of Finance population projections based on high, medium, and low growth rates (Sleeter et. al. 2017,). For each growth rate projection, ten variants were provided that incorporated random variation in the future spatial footprint of development.

Additional vegetation characteristics data for the Sierra Nevada, in the form of fire regime condition class (*FRCC*) variables designed to measure the divergence of vegetation structure and composition from historical conditions (Hann et al 2008, Laverty and Williams 2000), were provided by the US Department of Agriculture's Forest Service Region 5 using the same methodology as the LANDFIRE project (Keane et al 2007, www.landfire.gov). *FRCC* classes 2 and 3 were combined (indicating ≥33% departure from historical conditions (Holsinger et al 2006, Keane et al 2007)) and aggregated to indicate fractional coverage of the 1/16th-degree lat/lon grid used here. Fractional data were then normalized to provide a continuous variable not bounded by [0,1] as:

$$FRCC23_i = log((f23_i) / (1-f23_i))$$

where $f23_i$ is the fractional vegetated area characterized as *FRCC* class 2 or 3 in grid cell *i*. Fuels management scenarios were constructed by randomly converting 30 m pixels within each federal land management unit from *FRCC* classes 2 and 3 to *FRCC* class 1 (i.e. approximating historical conditions prior to the era fire suppression, with more open forest canopies, shorter fire rotations, and less severe fire (less biomass burned and less mature tree mortality)). Historical conditions are defined relative to specific vegetation types at a 30 m resolution by U.S. Forest Service using the same methodology as the Landfire project (www.landfire.gov).

Scenarios reported here examined converting, respectively, approximately 50% and 90% (R50 and R90 management scenarios) of the potentially treatable forest area to *FRCC* 1. Note that,

while this is a large area, it is considerably less than 50% or 90% of the total area with native vegetation. Treating ~50% of the potentially treatable area corresponds to less than 30% of the total vegetated area, and 90% of the potentially treatable area corresponds to less than 45% of the total vegetated area. Even so, the R50 management scenario effectively would triple the area currently with historical fuels conditions, while the R90 management scenario effectively more than quadruples the area with historical fuels conditions. In practice, treatments at this scale would require a combination of mechanical tree removal and fires actively managed for fuels reduction objectives.

2.1.4 Historical Climate and Hydrologic Data

A common set of gridded historical (1915–2015) climate data including daily maximum and minimum temperature and precipitation (P)—as well as potential (PET) and actual (AET) evapotranspiration simulated with these climate data using the Variable Infiltration Capacity model (VIC)—were obtained from the Livneh Research Group at the University of Colorado, Boulder (Livneh et al 2013). Climatic water deficit (CWD) was then calculated from *PET* and *AET* (*CWD* = *PET* - *AET*). Average temperature (T) was calculated as the average of daily maximum and minimum temperature. Daily values were cumulated to monthly values for all variables, as well as cumulative water-year (October - September) totals for *CWD* (*CWD0* = current water year, *CWD1* = previous water year). Seasonally averaged March - May and June - August (*Tmam, Tjja*) temperatures were calculated for each grid cell, and also a regionally average June - August temperature index (*TRjja*). In addition, we calculated long term mean and standard deviation for *AET* and *CWD* (*AET.mu*, *AET.sd*, *CWD.mu*, *CWD.sd*) for each grid cell for the 1961-1990 reference period.

2.1.5 Simulated Climate and Hydrologic Data

We obtained gridded downscaled climate simulations for 1950-2099 from four global climate models using two emissions scenarios (Representative Concentration Pathway (RCP) 4.5 and 8.5, see IPCC AR5 WG1, 2013) via Scripps Institution of Oceanography, including global models from Centre National de Recherches Météorologiques (CNRM-CM5, see Voldoire et al 2011), the Canadian Centre for Climate Modeling and Analysis (CanESM2, see Christian et al 2010, Arora and Boer 2010), the United Kingdom Met Office's Hadley Center (HadGEM2-ES, see Collins et al 2008), and the University of Tokyo's Center for Climate System Research (MIROC5, see Watanabe et al 2010). These climate models were selected by Fourth Assessment colleagues (Pierce et. al. 2018) who applied a set of filters at global, regional, and California scales to obtain models that realistically represent variability for California in selected hydrologic variables and the climatological drivers of that variability. RCP 4.5 describes a global scenario where greenhouse gas emissions begin to decline by mid-21st century and level off by 2080, while RCP 8.5 describes a world where emissions rise rapidly in coming decades. Climate scenarios were downscaled to a 1/16 degree lat/lon grid using the Localized Constructed Analogs (LOCA) statistical downscaling methodology (Pierce, Cayan, and Thrasher 2014). These climate scenarios were used to drive the VIC hydrologic model, resulting in the same set of variables as described above for historically observed climate. Because lagged relationships were examined between wildfire and climate up to two water years preceding a fire event, the projections allowed examination of 147 years, from 1953 through 2099.

2.1.6 Topographic Data

Topographic data on a 1/16-degree grid were derived from the GTOPO30 Global 30 Arc Second (~1km) Elevation Data Set (Mitchell et al 2004, Gesch and Larson 1996, Verdin and Greenlee 1996). We calculated mean and standard deviation of elevation, slope, and aspect for each grid cell.

2.2 Modeling

2.2.1 Model: Fire Presence

Probability of large (>400 ha) fire presence or absence was modeled fitting a spatially explicit logistic regression model to land surface characteristics (topography, population, vegetation fraction) and climate using a logistic regression model. A generalized linear model with binomial errors was fit using the *glm()* function in R. The model specification is described as follows:

Let $b_{ij} = 1$ denote the presence of one or more large (> 400 ha) fires and $b_{ij} = 0$ the absence of a large fire, burning for each grid cell i and month j. Then b_{ij} is a random variable with the Bernoulli distribution, and the probability p_{ij} of a large fire is:

$$p_{ij} = \exp(\lambda_{ij}) / (1 = \exp(\lambda_{ij}))$$

and λ_{ij} is the linear predictor

$$\lambda_{ij} = \beta_o \times g(AET.mu_i, CWDmu_i) + \sum \beta_m \times g(AET.mu_i, CWDmu_i) \times q_m(X_{mij}) + \sum \beta_m \times X_{mij}$$

where X_{mij} is the mth explanatory variable for location i and month j (Table 1), $g(AET.mu_i, CWDmu_i)$ denotes a semiparametric function g of the interaction between long term average evapotranspiration and long-term average climatic water deficit, $q_m(X_{mij})$ denotes a parametric or semiparametric function of the mth explanatory variable (see Hastie et al 2001), and β are estimated parameters. Semiparametric functions here are splines and thin-plate splines expanded into basis functions that can be used linearly in the regression (Preisler and Westerling 2007). Similar mixed parametric and semiparametric models for large fire presence have been used by the author and others for both seasonal forecasting and climate change impact assessment (Preisler and Westerling 2007, Preisler et al 2008, Preisler et al 2011, Westerling et al 2011a&b). Long-term average climatic water deficit and evapotranspiration have together been shown to best describe the occurrence of coarse vegetation types on the

landscape (Stephenson 1998), and coarse vegetation types and their climatic context strongly condition the response of fire regimes (frequency, extent and severity) to climatic variability (Westerling 2009, Westerling et al 2009, Krawchuck and Moritz 2011). Prior fire presence/absence models using cumulative moisture deficit are described in Westerling et al (2011a&b).

Table 1. Logistic regression model specification for large fire presence

$= \beta_m \times g(AET.mu_i, CWDmu_i) + \sum \beta_m \times g(AET.mu_i, CWDmu_i) \times q_m(X_{mij}) + \sum \beta_m \times X_{mij}$		
for $\sum g(AET.mu_i, CWDmu_i) \times q_m(X_{mij})$ terms		
		description
$q_m(X_{mij}) =$	$q(CWD_{ij})$	basis spline of cumulative monthly climate water deficit
	$q(T_{ij})$	basis spline of average temperature
	$q(VFR_{ij})$	basis spline of vegetation fraction
	$q(POP_{ij})$	basis spline of population
	$CWD0_{ij}$	cumulative water year climate water deficit
	$CWD1_{ij}$	lagged cumulative water year climate water deficit
	AET_{ij}	cumulative monthly actual evapotranspiration
	Emu	mean elevation
	$M_{78} * TRjja_{ij}$	Regional JJA temperature interacted with a factor for month = July or August

	M	factor for month of the year
for $\sum \beta_m \times X_{mij}$ terms		
		description
X_{mij} =	$CWD_{ij} * AET_{ij}$	interaction between cumulative monthly climate water deficit and cumulative monthly actual evapotranspiration
	FSR	standardized fraction of grid cell in federal or state protection responsibility areas
	$Tmam_{ij}$	average MAM temperature

Model specifications were tested by sequentially adding and removing explanatory variables X_m and comparing Akaike Information Criterion scores (AIC) (Akaike 1974 & 1981). The model with the lowest AIC was retained. Where differences in AIC were small (close to 2), expert judgement and parsimony guided model selection. AIC is a measure of goodness of fit that penalizes increasing model complexity and is not distorted by spatially autocorrelated variables. Model specifications tested for large fire presence/absence were based on models used in Westerling et al (2011a), the primary differences being a change to a finer spatial scale (from a 1/8 degree to a 1/16 degree lat/lon grid) with a larger minimum fire size (from 200 ha to 400 ha), with the latter change due to the use here of MTBS fire histories rather than documentary fire histories.

Model validation was performed by calculating model parameters with a sample arbitrarily restricted to 1984-1999, applying parameters to the full thirty-year sample to estimate predicted fire presence, and comparing the correlations with correlations for the model estimated with the full thirty-year sample. Spearman's rank correlations are reported throughout. Note that while the anthropogenic trend in temperature is present throughout the model estimation period, it is stronger in the second half of the record. To the extent that model skill is comparable across both periods for parameters estimated on the 1984-1999 data, we should have more confidence that this model can be used to simulate wildfires under additional near-future warming.

Fire presence/absence was simulated for both historically observed and simulated climate by repeated random draws from a Binomial distribution with probabilities p_{ij}.

2.2.2 Model: Fire Number

Following the methodology in Westerling et al (2011b), a Poisson lognormal probability model was fit to fire numbers f_{ij} observed per month i and grid cell j where $b_{ij} > 0$ and linear predictor

$\theta\theta_{ij} > -7.79$, an arbitrary threshold below which all observed $f_{ij} < 2$, using the *rplnmle()* function in the *degreenet* library in R (Jones and Handcock 2003). Random Poisson lognormal draws were truncated not to exceed 2 in all the simulations, since over the historically observed period there were no instances of more than two large fire ignitions (observed $0 \leq f_{ij} \leq 2$), and even these were rare (only five instances over all of California in 30 years).

2.2.3 Model: Fire Size

Extreme values over a fixed threshold—such as wildfire sizes exceeding 400 ha—can be described statistically with a generalized Pareto distribution (GPD) (Coles 2001). A growing body of work indicates that wildfire area burned in large fires follows a heavy-tailed Pareto distribution in a diverse array of ecosystems (Strauss et al 1989, Moritz 1997, Malamud et al 1998, Ricotta et al 1999, Cumming 2001, Song et al 2001, Zhang et al 2003, Malamud et al 2005, Ramesh 2005, Holmes et al 2008, Preisler et al 2011, Westerling et al 2011b). Fires sizes over 400 ha were modeled here with a generalized Pareto distribution fit to the logarithm of area burned, from MTBS fire records, with covariates using the gpd.fit() function in the ismev library in R, derived from Coles (2001), as in Westerling et al (2011b).

The GPD is described by three parameters: threshold u, scale σ, and shape α such that the expected area burned A_{ij} for a fire at a given time and place takes the form:

$$\mathbf{E}(\log(A_{ij}) \mid A_{ij} > u) = \sigma\sigma(X_{mij}) / (1 - \alpha\alpha(X_{mij}))$$

where σ and α can be specified as functions of covariates X_m.

The threshold u used for defining extremes should be high enough that the remaining data are legitimately extreme values, but low enough to maximize the size of the data set. A rule of thumb is to choose a threshold where the mean of the sample defined by that and higher thresholds is a linear function of the threshold value (Coles 2001). Prior work with fire histories in California (Holmes et al 2008, Westerling et al 2011a, Preisler et al 2011) indicates a minimum threshold of 200 ha or greater is appropriate. The 400 ha threshold used here was imposed by the lower limit reported in the MTBS fire history data source.

Two GPD models were estimated for simulating fire sizes in California: one fit to fire histories for federal forest areas in the Sierra Nevada, and one fit to fire histories for the rest of the state. Separating out Sierra Nevada forests facilitates further use of these models for informing climate adaptation planning in the Sierra Nevada, where the US Department of Agriculture's Forest Service Region 5 has provided historical data and fuels management scenarios—expressed as changes in FRCC categories at 30m scale—describing how fuel densities may be reduced to modify future fire probabilities. An array of climate and topographic variables, as well as FRCC23, were tested as covariates for both the shape and scale parameters for GPD models in the Sierra Nevada and the rest of the state, using AIC to compare different model specifications.

The threshold used in this study (400 ha) is double the level used in prior studies in California and elsewhere (Holmes, Huggett and Westerling 2008, Westerling et al 2011a, Westerling et al

2011b, Alvarado et al 1998). The rule of thumb is to create a mean excess plot for a fire history and to select by visual inspection a threshold above which the plot is linear (Coles 2001). Using a larger threshold here means using a smaller sample of fires to estimate the distribution, but the excluded fires are the smallest fires that provide the least information about the behavior of the tail of the distribution.

2.3 Fire Duration

Note that the fire history used to build these models provides the discovery date and the total burned area but does not provide a day by day progression of burned area. Fire spread rates can vary greatly with weather conditions and suppression over the course of a fire. Even with accurate estimates of fire start and fire duration, we would not know when most of the area burned. Deciding precisely when a fire is over is problematic as well, since official control and out dates can be somewhat arbitrary and are influenced by administrative as well as meteorological factors. Consequently, we do not attempt to define or model fire duration here. However, since the fire start dates modeled here are typically date of discovery, and fires are only included if they exceed 1000 acres, it is likely that spread rates are often very significant at or soon after the date of discovery, or else the fire would be extinguished before it could reach the 400 hectare threshold to be included in the fire history used here.

2.4 Summary of Scenarios

Future scenarios described here were defined by two concentration pathways for greenhouse gasses (RCP 4.5 and 8.5), four climate model runs with varying sensitivities to greenhouse gas forcing as well as different realizations in background climate variability (CanESM2, CNRM-CM5, HadGEM2-ES, and MIROC5), three population growth scenarios (low, medium and high) with ten spatially stochastic variants each, and recent historical FRCC. This resulted in an initial 240 scenarios (2 x 4 x 3 x 10). For each of these, 100 random draws were made from the combined binomial, Poisson lognormal, and GPD models described above to capture a broader range of variability in wildfire burned area, the impacts from which are dominated by a small number of low-probability extreme events. The result is 24,000 scenarios, each covering 9922 grid cells for 1764 months (12 months x 147 years (1953 to 2099)). This resulted in 42,336,000 maps of statewide monthly fire activity for each variable considered (i.e., large fire presence, number, extent, …). In addition, fire activity was simulated for each of two fuels management scenarios for Sierra Nevada forests, where approximately 50% and 90% of altered fuels considered by the Forest Service to be amenable to treatment (thinning and burning) were treated, in combination with the two emissions pathways, the same four GCMs, and one medium population scenario. The result was an additional 1,600 scenarios (2 x 2 x 4 x 1 x 100), resulting in 2,822,400 additional maps for each variable.

These data were further aggregated to produce annual area burned in all fires originating within a grid cell. Where annual area burned exceeded the average vegetated area of a grid cell, excess burned area was arbitrarily allocated proportionately to all the surrounding grid cells.

Where this implied large fires burning into others' footprint, total area burned in the combined fires was reduced by the amount of overlap that exceeded the burnable area, reflecting limitations imposed by the availability of fuels.

Similarly, 1000 draws were made from the combined binomial, Poisson lognormal, and GPD probability models driven by historically observed climate, for comparison with observed fire activity. Monthly and annualized simulated fire presence and area burned were aggregated statewide, averaged over 1000 simulations, and correlated with observed. In addition to correlations, we also graphically compared simulated to observed area burned. Because the low probability of extreme events combined with a fat-tailed probability distribution means that observations are highly variable for a given level of fire risk, multiple similar simulations were grouped and compared to observations as follows: observed and simulated monthly statewide aggregate area burned were ranked according to the average simulated value for each month, and grouped into 30 bins each corresponding to 12 months with similar predicted burned areas. Box plots were graphed for both observed and simulated monthly statewide area burned in each bin (with 12 observed values versus 12,000 simulated values in each bin).

3: Results

3.1 Logistic Regression for Large Fire Presence (Binomial Model)

The best model specification for fire presence incorporated land surface characteristics such as population, vegetation fraction, fractional area in state and federal protection responsibility, and elevation, with monthly and water year climate water deficit, monthly and seasonal temperature, actual evapotranspiration, and month of the year (Table 1).

Monthly fire presence simulated using historical (1984 - 2013) climate aggregated statewide and averaged over 1000 simulations was highly significantly correlated with observed fire presence (rho = 0.84, p-value < 2.2e-16). Cross-validated simulated fire presence was also highly significantly correlated (rho = 0.83, p-value < 2.2e-16). Annual simulated fire presence was significantly correlated with observed (rho = 0.55, p-value = 0.002), as was cross-validated simulated fire presence (rho= 0.46, p-value = 0.011).

3.2 Conditional Model for Fire Number (Poisson Lognormal Model)

A Poisson lognormal model specification was chosen that closely mimicked historical occurrence of multiple large fire ignitions, conditional on $\boldsymbol{\theta\theta}_{ij}$:

for $b_{ij} = 1$ and $\boldsymbol{\theta\theta}_{ij} \leq -7.79, f_{ij} = 1$

for $b_{ij} = 1$ and $\boldsymbol{\theta\theta}_{ij} > -7.79, f_{ij} \sim$ Poisson lognormal with mean = -4.94 and standard deviation = 0.3

for $b_{ij} = 0, f_{ij} = 0$

Historically, five occurrences of large fire ignitions in the same month and location were observed. Across 1000 simulations over the state using historical climate for 1984-2013, the average occurrence of multiple ignitions was approximately 5.

3.3 Conditional Area Burned (GPD Model)

In the Sierra Nevada, none of the covariates offered significant improvements over a stationary model for the GPD shape parameter, while the scale parameter was modeled as a function of CWD_{ij}, $Tjja_{ij}$, and $FRCC23_j$. For the rest of the state, the best GPD model selected with AIC had the scale parameter as a function of *Tjja* and *TRjja*, and the shape parameter as a function of a thin plate spline for $AET.mu_i$ and $CWD.mu_i$ interacted with monthly CWD_{ij}. These models result in reasonable fits between observed and simulated distributions of large fire sizes (Figure A1).

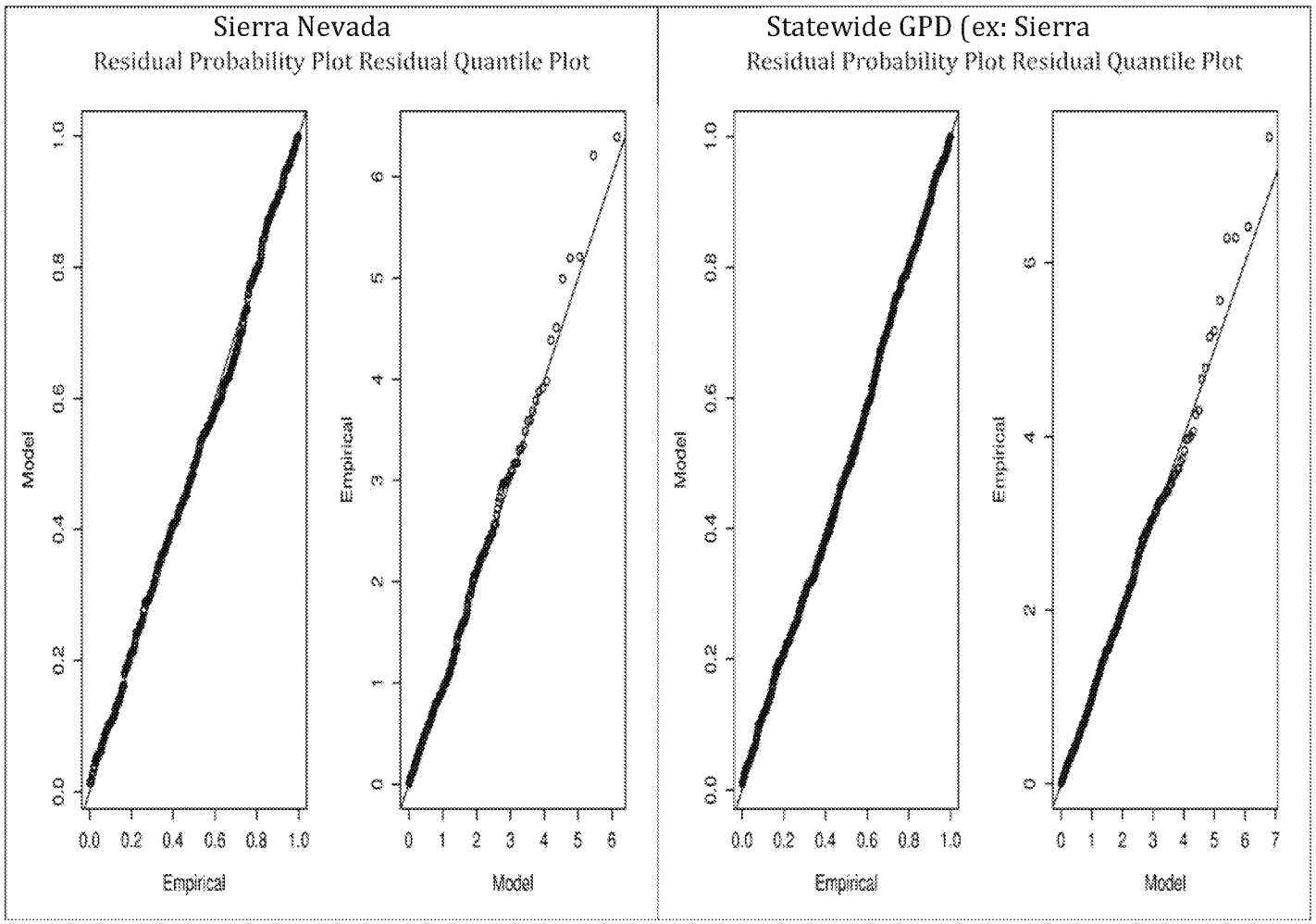

Figure A1: Residual Probability and residual quantile plots for Sierra Nevada (left) and Statewide, excluding Sierra Nevada (right).

Thus, for both the Sierra Nevada and the rest of the state, conditional area burned varies with seasonal and interannual climate, driven by the scale parameter (in the Sierra Nevada and the rest of the state) and the shape parameter (in the rest of the state). While the statewide model excluding the Sierra Nevada still includes very diverse fire regimes, the response of the shape

parameter in that model to current month *CWD* varies with the interaction between long term average *AET* and long term average *CWD*. As noted above, the interaction between long term average *AET* and *CWD* is a good proxy for coarse vegetation type (Stephenson 1998). The shape of the statewide fire size distribution is varying with coarse vegetation characteristics in each grid cell, reflecting differences in how fire size responds to climate in different vegetation types.

3.4 Historical Area Burned Simulations

Monthly area burned simulations, incorporating all binomial, Poisson lognormal, and GPD models, aggregated statewide and averaged across 1000 simulations, were highly significantly correlated with observed monthly area burned (rho = 0.78, p-value < 2.2e-16). Average annualized area burned simulations aggregated statewide were also significantly correlated with observed annual burned area (rho = 0.62, p-value = 0.0003).

The extremely large fires that drive most wildfire impacts are low probability events in any given month and location, even when conditions historically have been conducive to fire, making direct comparisons with expected burned area difficult. However, even binning over a relatively small number of months (12) and comparing to a sufficient number of simulations to describe the full distribution of expected outcomes serves to demonstrate some strengths and weaknesses of this modeling approach (Figure A2).

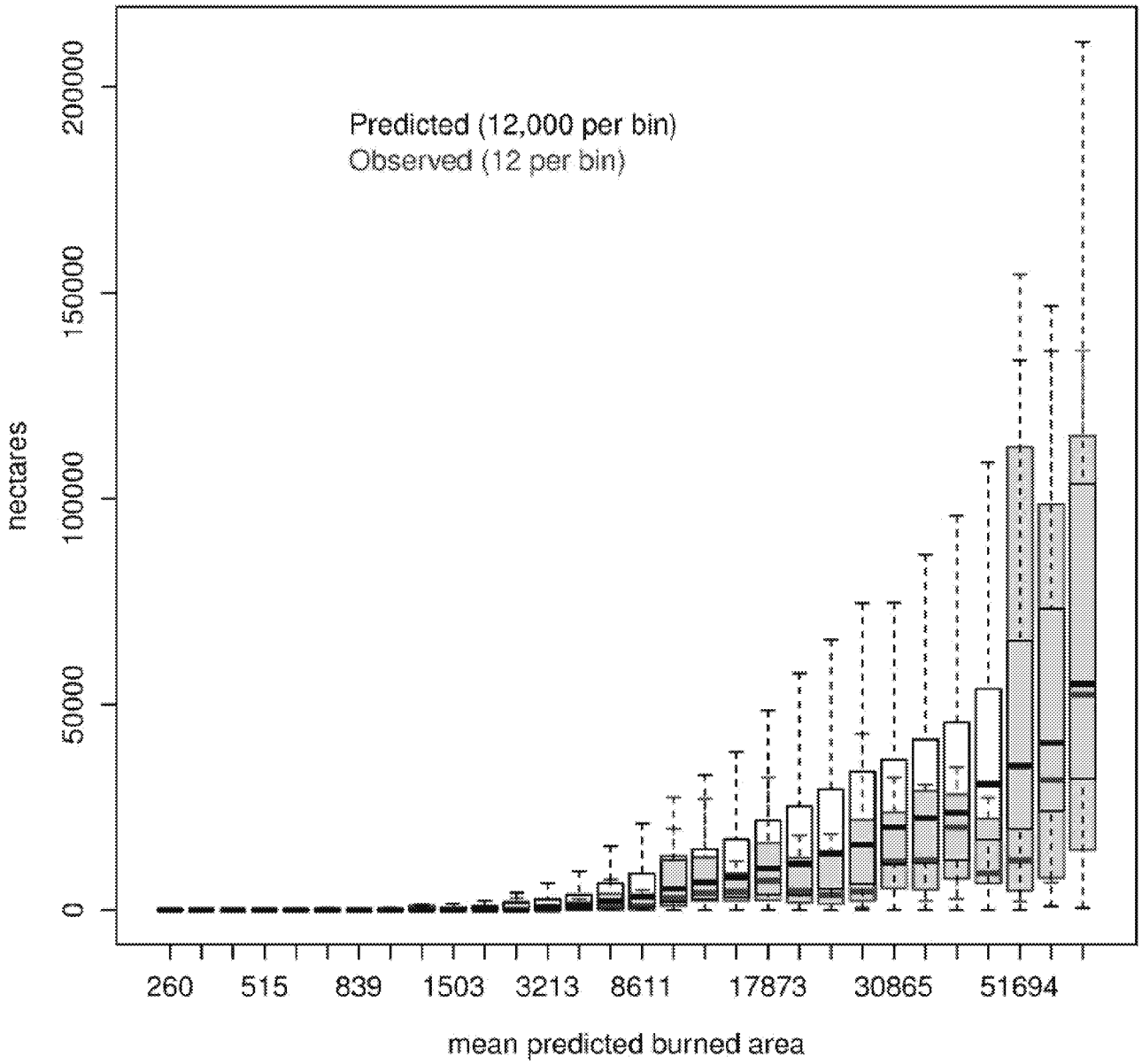

Figure A2: Binned monthly statewide predicted area burned in hectares (black boxplots) versus observed area burned (red boxplots). Monthly data for 30 years were aggregated statewide, ranked, and clustered in equal-sized bins corresponding to 12 ranked months. Sample size per observed bin is 12 observations of statewide area burned. For each predicted bin, 1000 simulations are included for each month, resulting in 12,000 member samples for each observed binned boxplot. Boxes show interquartile range, bold bars show medians, and whiskers denote 1.5 times the interquartile range.

For months with statewide area burned below about 15,000 ha, observed and simulated area burned appear quite similar, reflecting the tendency of the seasonal cycle to limit area burned in

a predictable way during cooler, wetter months of the year. As predicted area burned increases, the influence of interannual variability in climate on observed fire increases. While there is still a strong tendency for the observed and simulated area burned to increase together, the effects of the relatively small sample size for observed very large fires and the difficulty in reliably modeling extremes in fire activity influenced by both clustering in ignitions due to factors such as dry lightning events, and to influences of meteorological factors such as wind events on the growth of fires, become apparent (Figure A2). Despite these limitations, observed and simulated area burned were highly correlated, and the combined probability models explained about 31% of inter-annual variability in area burned statewide. The fact that observed area burned distributions for the largest bin sizes were similar to the simulated areas is encouraging, since these months drive most of the interannual variability in wildfire.

3.5 Projected Area Burned Simulations

The greatest differences in simulated future area burned were between different emissions scenarios, rather than between climate models, while population and vegetation fraction projections had negligible effects on projected burned area (Figures A3 & A4 show increases in emissions scenarios versus GCMs for mid-range population growth scenarios. High and low growth scenarios are not shown.) The greatest differences between RCP 4.5 and 8.5 were at the end of the 21st century, as increasingly divergent greenhouse gas concentrations drove warming that increasingly dried the vegetation that fuels wildfires. Composite maps of area burned by RCP combining simulations for all four GCMs (Figure A5) show the greatest increases in burned area are projected to be in forested areas of the state, particularly in the Sierra Nevada and southern Cascades in northern and central California, with annual average hectares burned in many parts of the Sierra Nevada doubling to quadrupling by end of century under the most extreme warming.

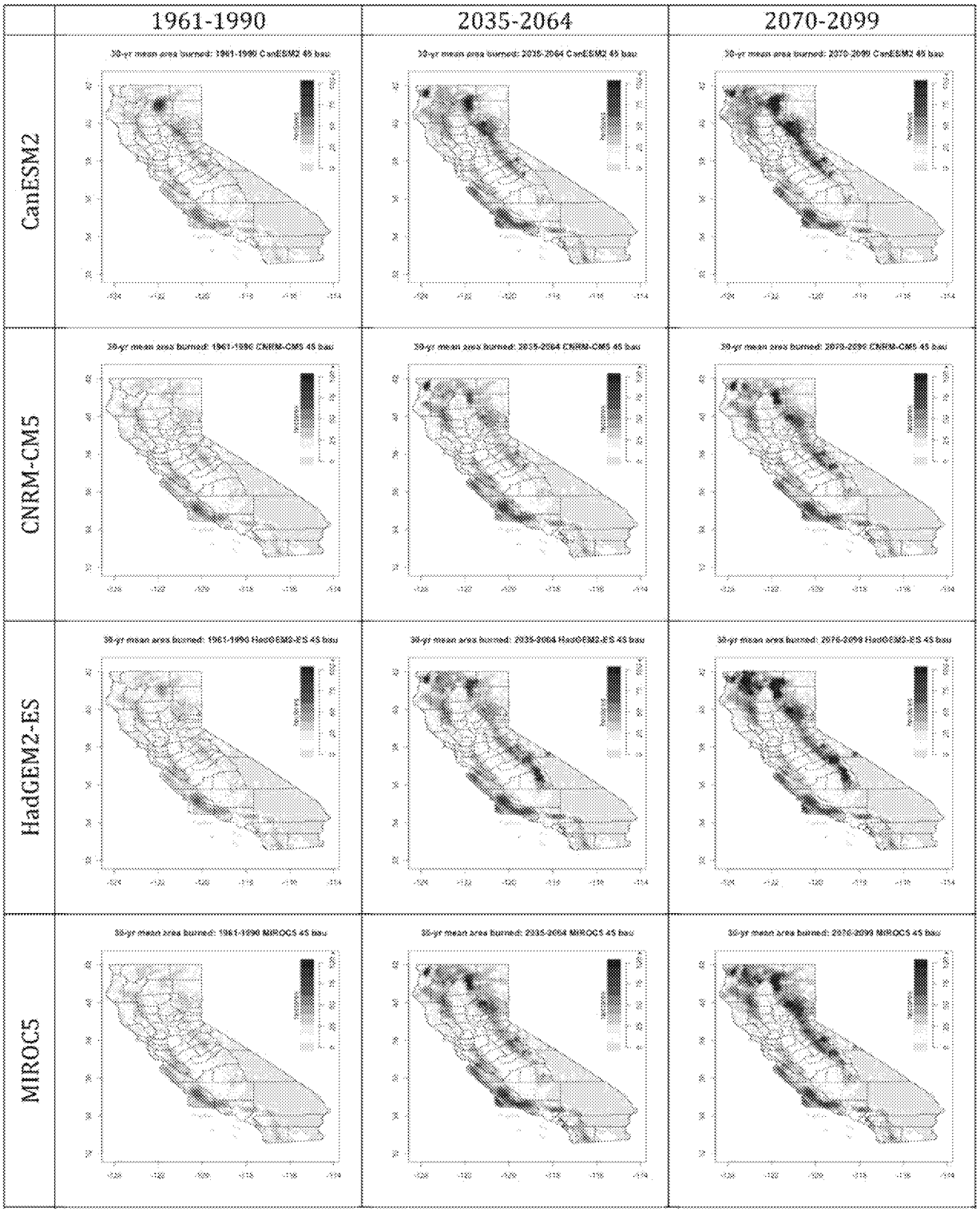

Figure A3: Average annual area burned by GCM and 30-year period for RCP 4.5, mid-range population growth.

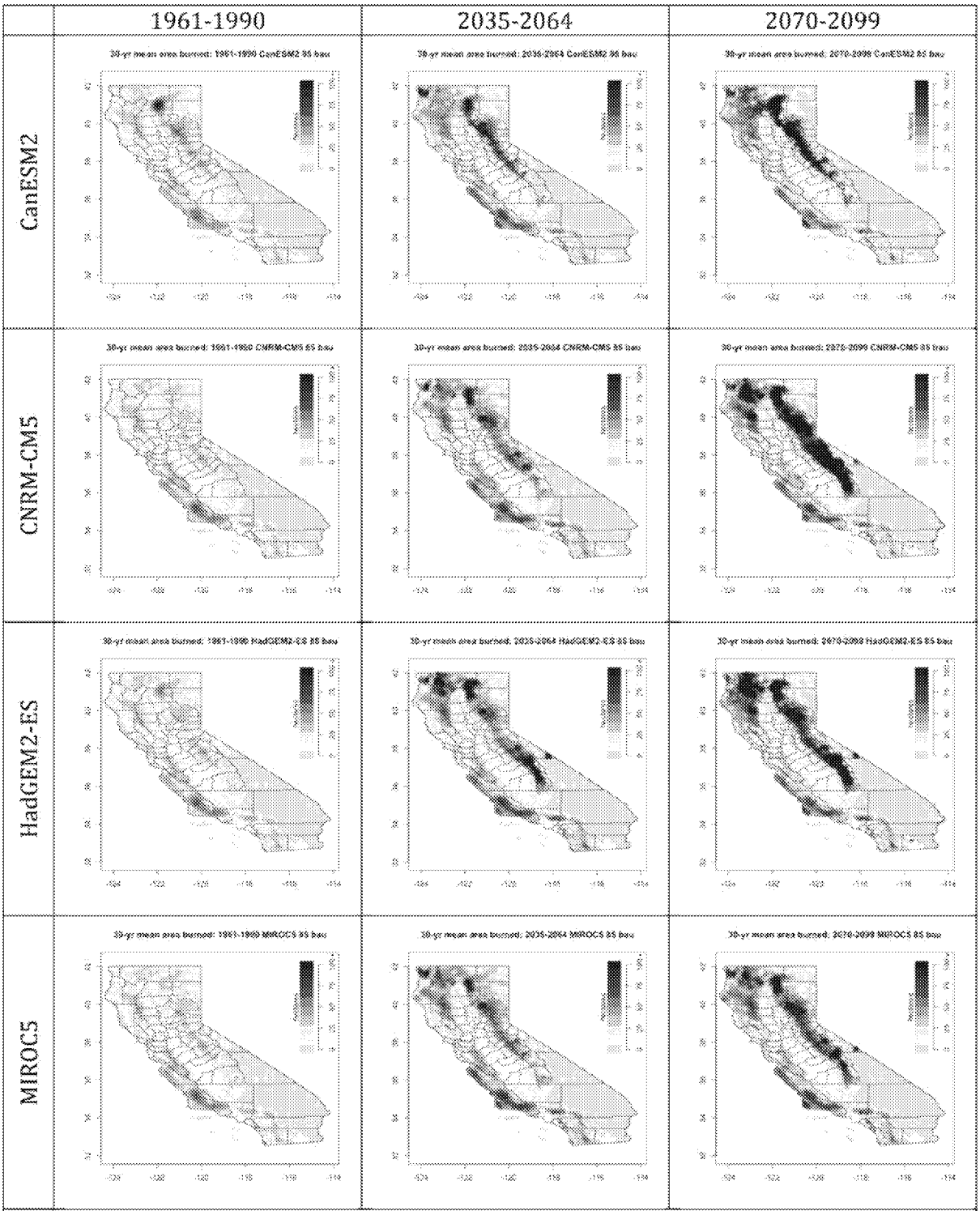

Figure A4: Average annual area burned by GCM and 30-year period for RCP 8.5, mid-range population growth.

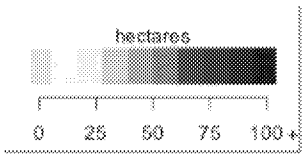

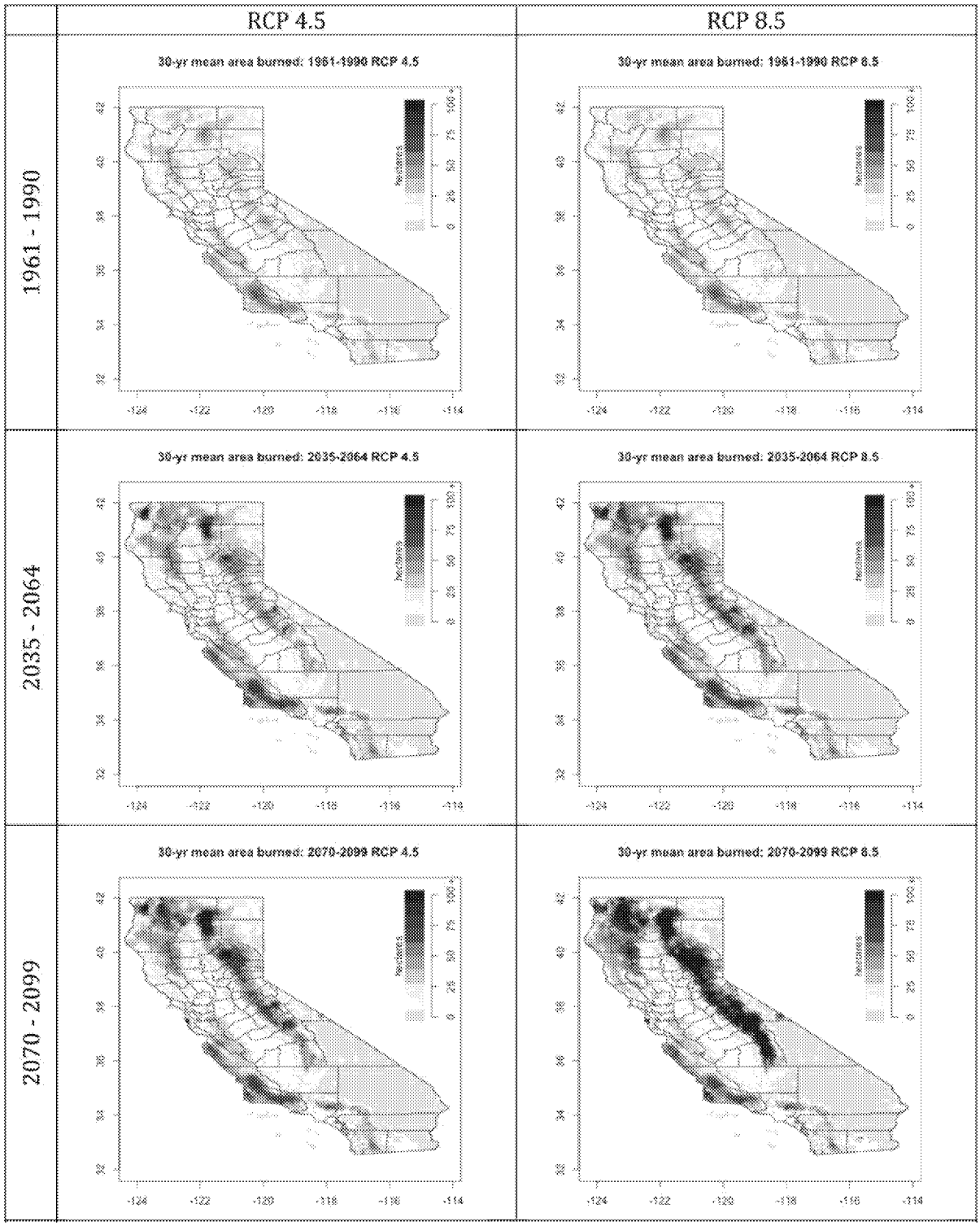

Figure A5: Average annual area burned composites: RCP 4.5 (left), RCP 8.5 (right), combining 4,320,000 simulations (30 years x 12 months x 1000 random draws x 4 GCMs x 3 population scenarios).

The fuel treatment scenarios explored here substantially mitigated increases in burned area over much of the Sierra Nevada. Without fuels reduction, large fires' area burned simulated under the RCP 4.5 scenarios (averaged across four GCMs) increased 48% by mid-21st century (Figure A6). The R50 and R90 management scenarios limited that increase to 33% and 28%, respectively. Similarly, by end of century, Sierra Nevada large fire burned area increased 120% over the 1961-90 period, and the R50 and R90 management scenarios limited the increase to 101% and 92% (Figure A7).

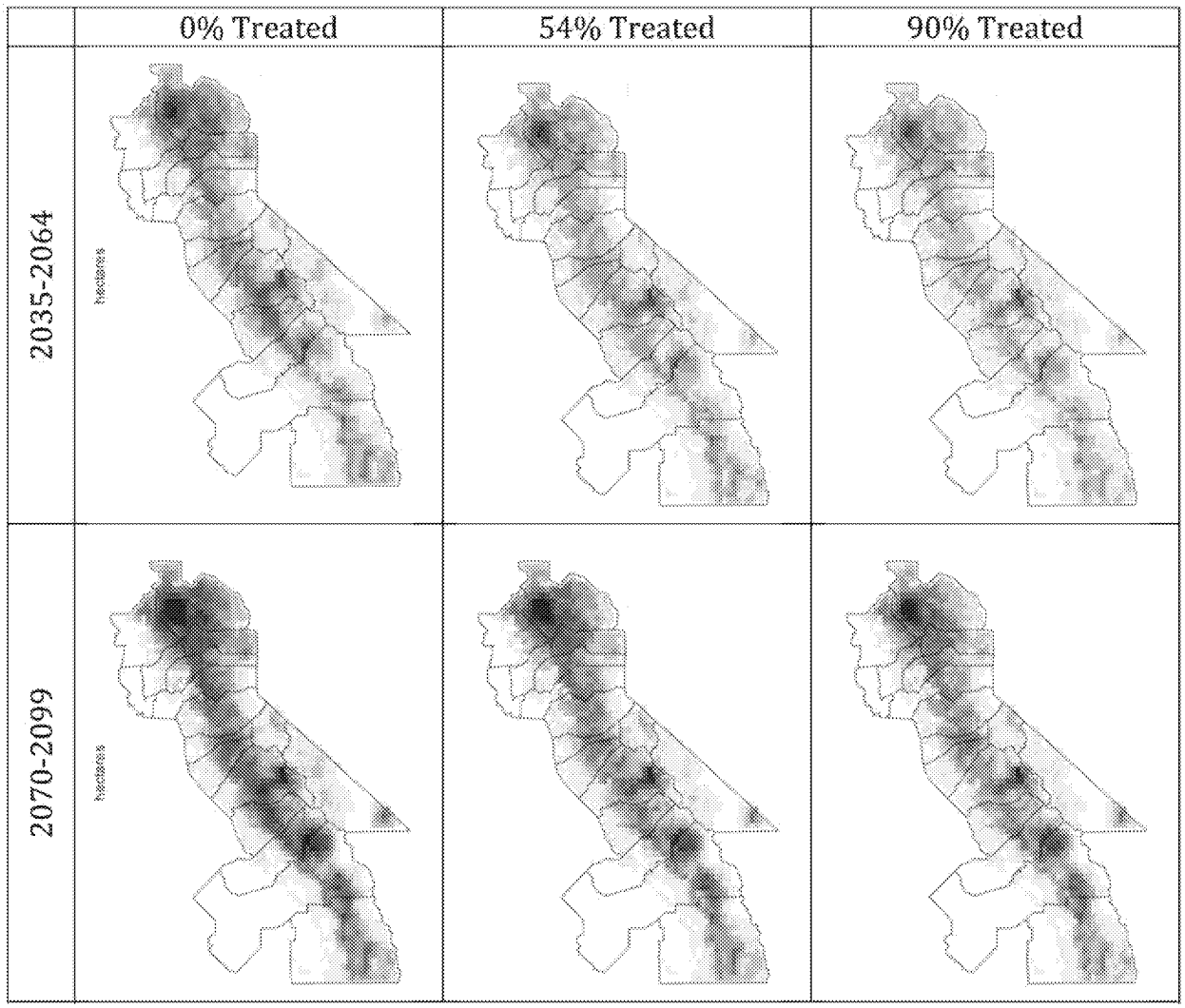

Figure A6: Average annual area burned composites for RCP 4.5: 0% (left), 54% (mid), and 90% (right) of altered forest fuels treated to restore pre/fire suppression fuel densities for mid/century (top) and end of century (bottom).

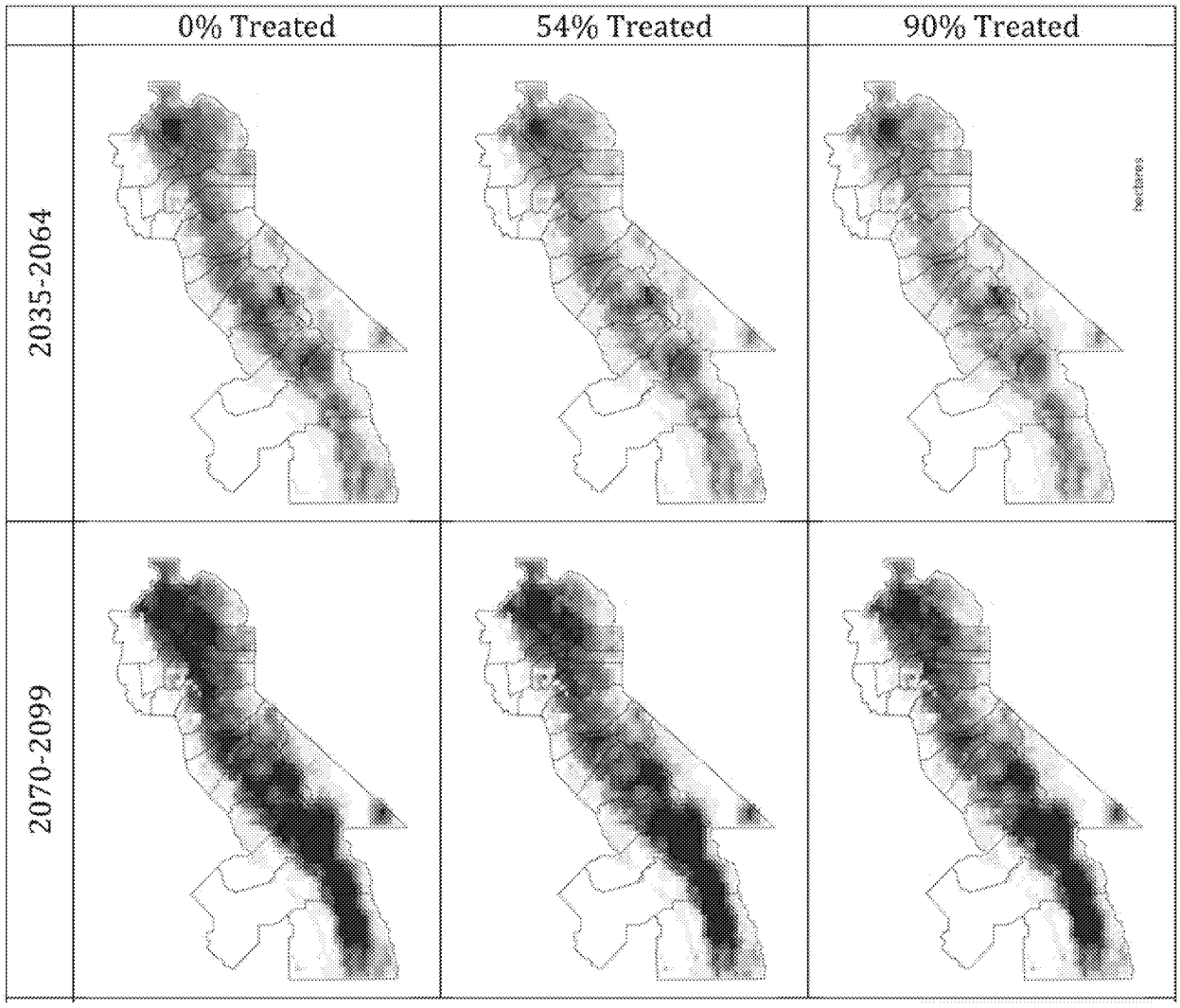

Figure A7: Average annual area burned composites for RCP 8.5: 0% (left), 54% (mid), and 90% (right) of altered forest fuels treated to restore pre/fire suppression fuel densities for mid/century (top) and end of century (bottom).

Pooling 100 randomly selected simulations from each of twelve scenarios (four GCMs and three population growth scenarios, no fuels management) for RCP 4.5 versus RCP 8.5 and aggregating annualized burned area statewide, a time series of the simulations shows that the greatest impact is on the frequency and size of extreme wildfire events (Figure A8). While the median annual statewide area burned for each RCP only begins to noticeably diverge late in century, there is a marked and increasing tendency toward greater extreme events under RCP 8.5 beginning early in the 21st century and rapidly accelerating after the mid-21st century. By end of century, the frequency of fires > 10,000 ha increases nearly 50%. Mean annual statewide area burned increases over 77%, while maximum statewide annual area burned increases by more than 178%.

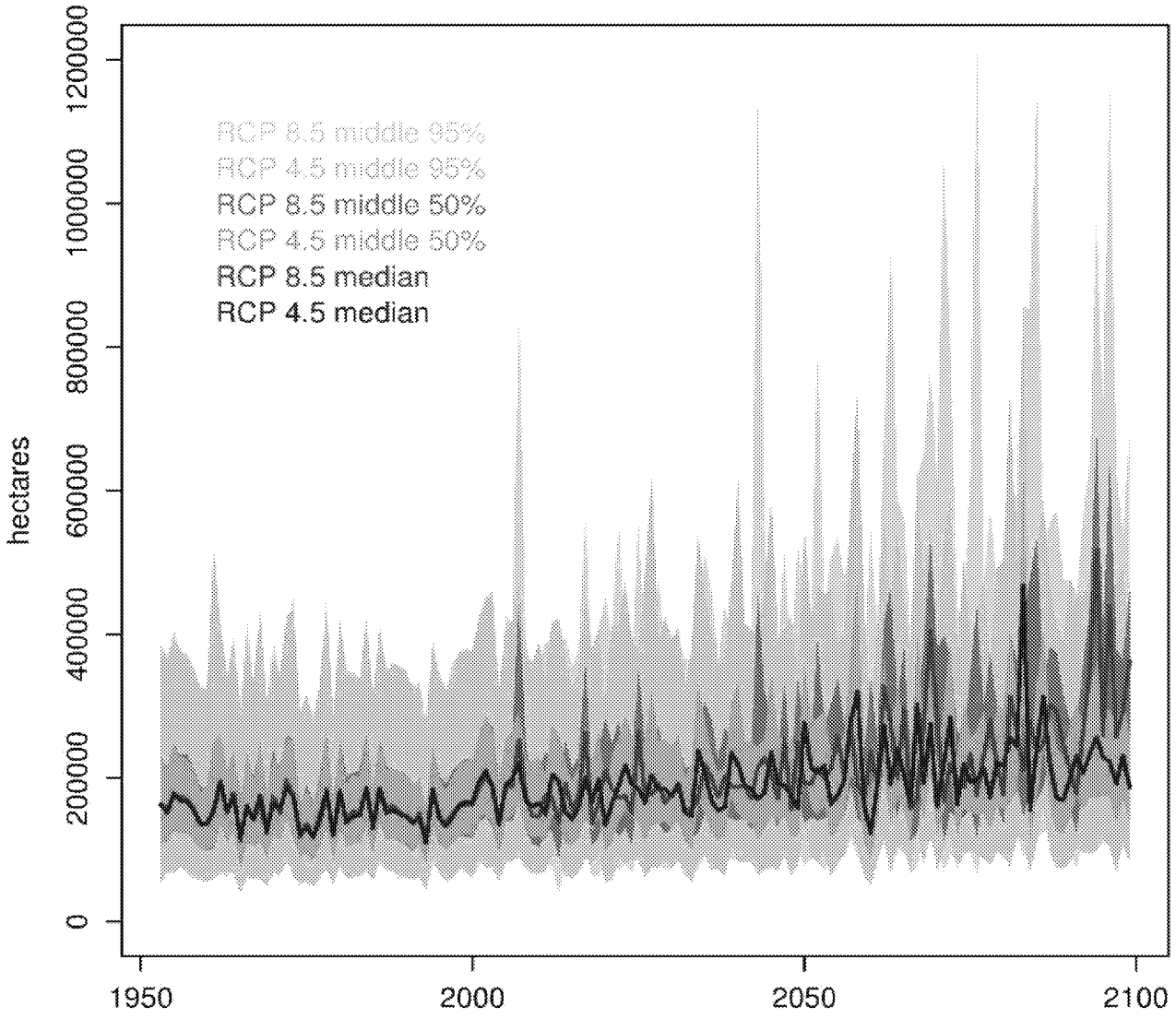

Figure A8: RCP4.5 vs 8.5 California Area Burned Quantities. Pooled simulations of annualized and aggregated statewide area burned for RCP 4.5 (blue) versus 8.5 (red). 100 randomly selected simulations from scenarios corresponding to each of four GCMs (CanESM2, CNRMKCM5, HadGEM2KES, MIROC5) and three population scenarios (low, mid and high range growth), resulting in 1200 simulations per year per RCP. Light shading shows middle 95%, dark shading shows middle 50%, and bold lines show median simulated values for statewide annual area burned.

3.6 Projected BA90 Severity Simulations

High severity area burned with ninety percent or greater basal area killed (BA90) was also modeled as a function of climate and land surface characteristics, with the addition of an independent variable for dead biomass from recent drought-related tree mortality in Sierra Nevada forests.

Due to the lack of data regarding the impact of dead and down heavy fuels, the modeling in Appendix B was limited to and movement of fine canopy fuels (pine needles) to the surface fuel layer in the next decade and a half. A postulated potential effect further into the future is that there might exist a risk of mass fires once a substantial quantity of dead and down heavy fuels (logs) cure out and sufficient fine fuels grow up around them to facilitate the spread of a fire severe enough to ignite these fuels (see for example Stephens et al 2018). There are no recent historical analogs for this situation that could provide data to estimate this postulated risk for Sierra Nevada forests.

Methods used were the same as those described above for total area burned (see Appendix B). In the absence of hard data, this part of the analysis engaged in scenario building, applying expert opinion guided by recent studies (Stephens et al 2018, Preisler et al 2017), and allowing for wide uncertainties to consider what the potential near term effects might be of recent tree mortality on subsequent high severity wildfire.

The fractional change in BA90 area immediately following the drought attributed to dessication of fine fuels (pine needles) due to prior tree mortality was relatively small and insignificant when considered from the perspective of the Sierra Nevada region as a whole, ranging from a less than 7% increase to less than 1%, averaged over all four global climate models. Most of the effect is concentrated where the highest mortality occurred, along the western slopes of the central and southern Sierra Nevada (Figures B2 - B6). However, significant t-tests for grid cells in these areas were no more numerous than what would be expected to be observed by chance. In other words, the effects on BA90 postulated for each scenario were small compared to the background variability inherent in the modeled system. This is not surprising, given the extreme fat tail distributions that characterize both fire size and high severity burned area.

4: Discussion

Increasing burned area with warming temperatures, particularly in montane forests of the northern two thirds of the state, and a greater share of burned area coming from extremely large fires, is consistent with recent experience in California and around the arid western United States. Westerling et al (2006) found that regional forest wildfire activity increased substantially since the mid-1980s, strongly associated with warmer temperatures, earlier spring snowmelt, and increased climatic water deficit. This mid-1980s date for noticeable increases in wildfire associated with temperature also roughly corresponds to the first date Barnett et al (2008) could detect a warming signal in western US temperature and hydrologic variables, and they attributed at least 60% of changes in winter temperature and snowpack to anthropogenic climate change. In a recent update on western wildfire trends, Westerling (2016) found that area burned in western forests in the decade through 2012 had increased by 1,271% over the 1973-1982 period, with Sierra Nevada forest area burned up by 324% over the same period, and statistically significant increases in burned area in non-forest vegetation across the region.

Abatzoglou and Williams (2016) attribute at least half the recent increases in western US forest burned area to anthropogenic warming.

The work presented here describes statistical models for simulating future individual fire events on a monthly time step on a grid of approximately 6 km × 6 km (16^{th} degree lat/lon) over

California. By constructing large libraries of simulations based on scenarios for future climate, population, and development footprint, we provide a resource for the analysis of the probability of extreme events and their impact on resources around the state. All too often, we are presented with future projections of fire as changes in mean fire occurrence, burned area, or related weather indices, when the majority of wildfire impacts are due to low probability, extreme fire events discrete in time and place. By working with simulations of individual large fire events, we can begin to understand how their spatial and temporal clustering uniquely impacts resources in ways that changes in mean area burned cannot reveal.

As vegetation type and fuel amount, structure, and continuity change in the future due to altered disturbance regimes (for example, changes in the frequency, seasonality, duration, extent and severity of wildfire and infestations by beetles and other pathogens) and climate, future wildfire activity and its response to climatic variability may change in ways that constrain further increases or even reduce wildfire activity in some ecosystems (Flannigan et al 2009, Krawchuk et al 2009, Batllori et al 2013). Many regional studies project spatially diverse changes in wildfire (e.g. Krawchuck et al 2009, Kitzberger et al 2017), and recent work demonstrates great spatial variability in wildfire responses to climate variability and trends (Krawchuk and Moritz 2011, Westerling 2016, Keyser and Westerling 2017, Kitzberger et al 2017). It is reasonable to expect that dramatic changes in climate and disturbance regimes may eventually change vegetation in ways that cannot be anticipated by statistical models like those employed here, which are informed by historical fire-vegetation-climate relationships in the context of current vegetation types and their fuels characteristics. Consequently, the modeling results here may overestimate late 21st century changes in wildfire, particularly in forested areas, because they implicitly assume vegetation and fuels characteristics remain constant. Changes by mid-century, which are no longer far off, seem more robust, because increases in fire frequency and extent by then are still well within the prehistorical range (Stephens et al 2007). Differences between RCP 4.5 and RCP 8.5 are also less extreme before mid- century, indicating they are relatively robust to near term changes in the trajectory of greenhouse gas emissions as well.

Simulations with large landscape-scale fuels treatments substantially reduced projected climate-driven increases in Sierra Nevada forest area burned. Fuels management implies reduced concentrated impacts from future extreme events at some cost in terms of carbon release and health impacts from chronic exposure to smoke from controlled burns (Silva et al 2017).

However, Liang et al (2018) show that comprehensive fuels treatments implemented gradually over the coming century are likely to increase net carbon storage in Sierra Nevada forests, while Liu et al (2017) estimate that prescribed fires may result in a net reduction of particulate emissions.

At the same time, recent western US droughts of the 21st century have been associated with greater temperature, precipitation, and climatic water deficit extremes than major 20th century droughts, with greater area burned and high severity burn fractions (fraction of burned area that is high severity) in drought affected areas, and greater subsequent insect-induced tree mortality following drought (Crockett and Westerling 2018). The recent California-centered extreme drought starting in 2012 in particular resulted in widespread tree mortality in Sierra Nevada forests (Stephens et al 2018). The standing dead vegetation is hypothesized to increase short term canopy fire probabilities, but may subsequently contribute to a reduction in canopy

density that reduces the probability of severe canopy fires, while the accumulation of large dead woody surface fuels may eventually increase the probability of mass fires in ways difficult to quantify with current fuel models (Stephens et al 2018). Current work seeks to estimate how the drought-induced dieback in Sierra Forests may interact with the consequences of fire and fuels management and accelerating climate change. Given the lack of observed analogues, this effort will require a sustained integrated effort involving fire and dynamic vegetation modeling informed by extensive field observations and validation against observed fire activity.

On-going extensions to this incorporate fire severity, emissions, and carbon budget variables with these scenarios, as well as integrating these statistical fire models with dynamic vegetation models to better understand feedbacks between vegetation and wildfire, and with habitat suitability models to understand how changing vegetation and wildfire may constrain future management options around endangered species habitats. Parallel, ongoing work also seeks to incorporate downscaled winds and relative humidity into fire simulations, to explore how changing wind regimes may interact with changes in precipitation variability and timing, as well as warming, to affect fire regimes in coastal California. The December 2017 Thomas fire in coastal southern California--the first wintertime megafire and, as of July 2018, the largest fire in state history—occurred against a backdrop of factors that may become more common in the future. These include a very wet previous winter that increased fine fuel growth; an extreme, multiyear drought that left standing dead fuels; record warmth combined with no significant precipitation from Fall into December that helped to desiccate fuels; and an extended high wind event at the time of the fire (https://climatefeedback.org/discussion-experts-california-wildfire-links-climate-change/). Understanding how these events may co-occur in the future will improve our assessment of the likelihood of future fire events of similar timing and magnitude and our ability to plan for more fire-safe communities.

This research includes simulations of extreme wildfire events under a comprehensive set of future climate, demographic, and ecosystem management scenarios to support assessment of potential future wildfire impacts—as well as adaptation strategies--on habitat quality, water resources, energy and transportation infrastructure, residential and commercial property losses, insurance markets, and public health under the California's Fourth Climate Change Assessment.

5: References

Abatzoglou, J.T. and Williams, A.P. 2016. Impact of anthropogenic climate change on wildfire across western US forests. Proceedings of the National Academy of Sciences, 113(42), pp.11770- 11775.

Akaike H. 1974. A new look at the statistical model identification. IEEE Trans Automatic Control. 19(6): 716-723.

Akaike H. 1981. Likelihood of a model and information criteria. J Econ 16(1):3-14.

Alvorado, E., D.V. Sandberg and S.G. Pickford. 1998. Modeling large forest fires as extreme events. Northwest Science 72: 66-75.

Arora, V.K. and G.J. Boer (2010) Uncertainties in the 20th century carbon budget associated with land use change, Global Change Biology, 16(12), 3327.3348.

Barnett, T.P., Pierce, D.W., Hidalgo, H.G., Bonfils, C., Santer, B.D., Das, T., Bala, G., Wood, A.W., Nozawa, T., Mirin, A.A. and Cayan, D.R., 2008. Human-induced changes in the hydrology of the western United States. Science, 319(5866), pp.1080-1083.

Batllori, E., Parisien, M.A., Krawchuk, M.A. and Moritz, M.A., 2013. Climate change-induced shifts in fire for Mediterranean ecosystems. Global Ecology and Biogeography, 22(10), pp.1118- 1129.

Brown, J.T.; Hall, B.L.; Westerling, A.L. 2004. The impact of twenty-first century climate change on wildland fire danger in the western United States: An application perspective. Climatic Change. 62: 365-388.

Christian, J.R., Arora, V.K., Boer, G.J., Curry, C.L., Zahariev, K., Denman, K.L., Flato, G.M., Lee, W.G., Merryfield, W.J., Roulet, N.T. and Scinocca, J.F., 2010. The global carbon cycle in the Canadian Earth system model (CanESM1): Preindustrial control simulation. *Journal of Geophysical Research: Biogeosciences*, *115*(G3).

Coles, S., 2001. An Introduction to Statistical Modeling of Extreme Values. Springer-Verlag, London, U.K., 208pp.

Collins, W.J., N. Bellouin, M. Doutriaux-Boucher, N. Gedney, T. Hinton, C. D. Jones, S. Liddicoat, G. Martin, F. O'Connor, J. Rae, C. Senior, I. Totterdell, S. Woodward, T. Reichler, J. Kim, 2008: Evaluation of the HadGEM2 model. Met Office Hadley Centre Technical Note no. HCTN 74, available from Met Office, FitzRoy Road, Exeter EX1 3PB http://www.metoffice.gov.uk/publications/HCTN/index.html

Crockett, J.L. & Westerling, A.L. 2018. Greater Temperature and Precipitation Extremes Intensify Western U.S. Droughts, Wildfire Severity, and Sierra Nevada Tree Mortality. *Journal of Climate* 31(1):341-354.

Cumming, S.G. 2001. A parametric model of the fire-size distribution. Canadian Journal of Forest Research 31:1297-1303.

Eidenshink J, Schwind B, Brewer K, Zhu Z, Quayle B and Howard S 2007 A project for monitoring trends in burn severity Fire Ecology 3 3–21

ESRI 1999 Arc Macro Language version 7.1.1: Developing ARC/INFO Menus and Macros with AML, for UNIX and Windows NT 2nd edn (Redlands, CA: ESRI Press) editors

Fann, N., Alman, B., Broome, R.A., Morgan, G.G., Johnston, F.H., Pouliot, G. and Rappold, A.G., 2018. The health impacts and economic value of wildland fire episodes in the US: 2008–2012.

Science of the Total Environment, 610, pp.802-809.

Flannigan, M.D., Krawchuk, M.A., de Groot, W.J., Wotton, B.M. and Gowman, L.M., 2009. Implications of changing climate for global wildland fire. International journal of wildland fire, 18(5), pp.483-507.

Ffolliott, P. F., G. J. Gottfried, and M. B. Baker (1989), Water yield from forest snowpack management: Research findings in Arizona and New Mexico, *Water Resour. Res.*, **25**(9), 1999– 2007.

Fried, J.S., Torn, M.S. and Mills, E., 2004. The impact of climate change on wildfire severity: a regional forecast for northern California. Climatic change, 64(1), pp.169-191.

Hastie, T. J., R. Tibshirani, and J. Friedman, 2001: The Elements of Statistical Learning: Data Mining, Inference, and Prediction. Springer, 533 pp.

Gesch, D.B. and Larson, K.S., 1996. Techniques for development of global 1-kilometer digital elevation models. Pecora thirteen, human interactions with the environment-perspectives from space, pp.20-22.

Hann, W., Shlisky, A., Havlina, D., Schon, K., Barrett, S., DeMeo, T., Pohl, K., Menakis, J., Hamilton, D., Jones, J. and Levesque, M., 2004. Interagency fire regime condition class guidebook. National Interagency Fire Center: Boise, ID) Available at http://www. frcc. gov/[Verified April 2008].

Hastie, T. J., R. Tibshirani, and J. Friedman, 2001: The Elements of Statistical Learning: Data Mining, Inference, and Predic- tion. Springer, 533 pp.

Holmes, T. P., R. J. Hugget and A. L. Westerling, 2008: "Statistical Analysis of Large Wildfires," Chapter 4 Economics of Forest Disturbance: Wildfires, Storms, and Pests, Series: Forestry Sciences, Vol 79. T.P. Holmes, J.P. Prestemon and K.L. Abt, Eds., XIV, 422 p. Springer. ISBN: 978-1-4020-4369-7

Holsinger, Lisa, Keane, R.E., Parsons, R., Karau, E., 2006. Development of biophysical gradient layers for the LANDFIRE prototype project. In: Rollins, M.G., Frame, C. (Eds.), The, LANDFIRE, Prototype Project: Nationally Consistent, Locally Relevant Geospatial Data for Wildland Fire, Management, USDA, Forest Service Rocky Mountain Research Station General Technical Report, RMRS-GTR-175.

IPCC AR5 WG1 (2013), Stocker, T.F.; et al., eds., Climate Change 2013: The Physical Science Basis. Working Group 1 (WG1) Contribution to the Intergovernmental Panel on Climate Change (IPCC) 5th Assessment Report (AR5), Cambridge University Press.

Jones, J. H. and Handcock, M. S. "An assessment of preferential attachment as a mechanism for human sexual network formation," Proceedings of the Royal Society, B, 2003, 270, 1123-1128.

Jones, G.M., Gutiérrez, R.J., Tempel, D.J., Whitmore, S.A., Berigan, W.J. and Peery, M.Z., 2016. Megafires: an emerging threat to old-forest species. *Frontiers in Ecology and the Environment*, *14*(6), pp.300-306.

Keane, R.E., Rollins, M. and Zhu, Z.L., 2007. Using simulated historical time series to prioritize fuel treatments on landscapes across the United States: the LANDFIRE prototype project. ecological modelling, 204(3-4), pp.485-502.

Keyser, A.R. & Westerling, A.L. 2017. Climate drives inter-annual variability in probability of high severity fire occurrence in the western United States. Environmental Research Letters. 12: 065003.

Krawchuk, M.A., Moritz, M.A., Parisien, M.A., Van Dorn, J. and Hayhoe, K., 2009. Global pyrogeography: the current and future distribution of wildfire. PloS one, 4(4), p.e5102.

Krawchuk, M.A. and Moritz, M.A., 2011. Constraints on global fire activity vary across a resource gradient. Ecology, 92(1), pp.121-132.

Kitzberger, T., Falk, D.A., Westerling, A.L. and Swetnam, T.W., 2017. Direct and indirect climate controls predict heterogeneous early-mid 21st century wildfire burned area across western and boreal North America. PloS one, 12(12), p.e0188486.

Kunzli, N., Avol, E., Wu, J., Gauderman, W.J., Rappaport, E., Millstein, J., Bennion, J., McConnell, R., Gilliland, F.D., Berhane, K. and Lurmann, F., 2006. Health effects of the 2003 Southern California wildfires on children. *American journal of respiratory and critical care medicine*, *174*(11), pp.1221-1228.

Laverty, L., Williams, J., 2000. Protecting people and sustaining resources in fire-adapted ecosystems—a cohesive strategy. Forest Service response to GAO Report GAO/RCED 99-65. USDA Forest Service, Washington, DC.

Lenihan JM, Bachelet D, Neilson RP, Drapek R (2008) Response of vegetation distribution, ecosystem productivity, and fire to climate change scenarios for California. Climatic Change 87(Suppl.), 215–230. doi:10.1007/S10584-007-9362-0

Liang, S., Hurteau, M.D. and Westerling, A.L., 2017. Potential decline in carbon carrying capacity under projected climate-wildfire interactions in the Sierra Nevada. *Scientific Reports*, *7*(1), p.2420.

Liang, S.; Hurteau, M.; Westerling, A.L. 2018 Implementing large-scale restoration treatments increases carbon storage and stability under projected climate-wildfire interactions in the Sierra Nevada. *Frontiers in Ecology and the Environment* 16(4): 207-212.

Liu, X., Huey, L.G., Yokelson, R.J., Selimovic, V., Simpson, I.J., Müller, M., Jimenez, J.L., Campuzano-Jost, P., Beyersdorf, A.J., Blake, D.R. and Butterfield, Z., 2017. Airborne measurements of western US wildfire emissions: Comparison with prescribed burning and air quality implications. *Journal of Geophysical Research: Atmospheres*, *122*(11), pp.6108-6129.

Livneh B., E.A. Rosenberg, C. Lin, B. Nijssen, V. Mishra, K.M. Andreadis, E.P. Maurer, and D.P. Lettenmaier, 2013: A Long-Term Hydrologically Based Dataset of Land Surface Fluxes and States for the Conterminous United States: Update and Extensions, Journal of Climate, 26, 9384– 9392.

Malamud, B.D., G. Morein, and D.L. Turcotte. 1998. Forest fires: An example of self- organized critical behavior. Science 281:1840-1842.

Malamud, B.D., J.D.A. Millington, and G.L.W. Perry. 2005. Characterizing wildfire regimes in the United States. Proceedings of the National Academy of Science 102(13):4694-4699.

Miller, J.D., Safford, H.D., Crimmins, M. and Thode, A.E., 2009. Quantitative evidence for increasing forest fire severity in the Sierra Nevada and southern Cascade Mountains, California and Nevada, USA. *Ecosystems*, *12*(1), pp.16-32.

Mitchell, K.E., Lohmann, D., Houser, P.R., Wood, E.F., Schaake, J.C., Robock, A., Cosgrove, B.A., Sheffield, J., Duan, Q., Luo, L. and Higgins, R.W., 2004. The multi-institution North American Land Data Assimilation System (NLDAS): Utilizing multiple GCIP products and partners in a continental distributed hydrological modeling system. Journal of Geophysical Research: Atmospheres, 109(D7).

Moritz, M.A. 1997. Analyzing extreme disturbance events: Fire in Los Padres National Forest. Ecological Applications 7:1252-1262.

MTBS Data Access: Fire Level Geospatial Data. (last accessed 2016, September). MTBS Project (USDA Forest Service/U.S. Geological Survey). Available online: http://mtbs.gov/direct-download.

National Research Council 2011. Climate stabilization targets: Emissions, Concentrations, and Impacts over Decades to Millennia. Washington, D.C.: The National Academies Press: 286 p.

Pierce, D.W., D.R. Cayan and B.L. Thrasher, 2014: Statistical Downscaling Using Localized Constructed Analogs (LOCA). Journal of Hydrometeorology, 15,2558-2585.

Preisler, H.K., A.L. Westerling, K. M. Gebert, F. Munoz-Arriola, T. Holmes 2011: "Spatially explicit forecasts of large wildland fire probability and suppression costs for California" International Journal of Wildland Fire, 20, 508-517.

Preisler, H. K., S. C. Chen, F. Fujioka, J. W. Benoit, A. L. Westerling, 2008: "Meteorological Model Applications for Estimating Probabilities of Wildland Fires," International Journal of Wildland Fire, 17:305-316. DOI: 10.1071/WF06162

Preisler, H.K., and A.L. Westerling 2007: "Statistical Model for Forecasting Monthly Large Wildfire Events in the Western United States" Journal of Applied Meteorology and Climatology, 46(7): 1020-1030. DOI: 10.1175/JAM2513.1

Ramesh, N.I. 2005. Semi-parametric analysis of extreme forest fires. Forest biometry, modeling, and information sciences. Vol (1): 1-10.

Ricotta, C., G. Avena, and M. Marchetti. 1999. The flaming sandpile: Self-organized cricality and wildfires. Ecological Modelling 119:73-77.

Schoenberg, F.P., R. Peng, and J. Woods. 2003. On the distribution of wildfire sizes. Environmetrics 14:583-592.

Silva, R.A., West, J.J., Lamarque, J.F., Shindell, D.T., Collins, W.J., Faluvegi, G., Folberth, G.A., Horowitz, L.W., Nagashima, T., Naik, V. and Rumbold, S.T., 2017. Future global mortality

from changes in air pollution attributable to climate change. *Nature Climate Change*, *7*(9), p.647.

Sleeter, B.M., Wilson, T.S., and Sherba, J.T., 2017, Land Use and Land Cover Projections for California's 4th Climate Assessment: U.S. Geological Survey data release, https://doi.org/10.5066/F7M61HFP. (https://www.sciencebase.gov/catalog/item/587fb408e4b085de6c11f389)

Smith, H.G., Sheridan, G.J., Lane, P.N., Nyman, P. and Haydon, S., 2011. Wildfire effects on water quality in forest catchments: a review with implications for water supply. *Journal of Hydrology*, *396*(1-2), pp.170-192.

Song, W., F. Weicheng, W. Binghong, and Z. Jianjun. 2001. Self-organized criticality of forest fire in China. Ecological Modelling 145:61-68.

Spracklen, D.V., Mickley, L.J., Logan, J.A., Hudman, R.C., Yevich, R., Flannigan, M.D. and Westerling, A.L., 2009. Impacts of climate change from 2000 to 2050 on wildfire activity and carbonaceous aerosol concentrations in the western United States. Journal of Geophysical Research: Atmospheres, 114(D20).

Stephens, S.L., Martin, R.E. and Clinton, N.E., 2007. Prehistoric fire area and emissions from California's forests, woodlands, shrublands, and grasslands. Forest Ecology and Management, 251(3), pp.205-216.

Stephens, S.L., Collins, B.M., Fettig, C.J., Finney, M.A., Hoffman, C.M., Knapp, E.E., North, M.P., Safford, H. and Wayman, R.B., 2018. Drought, Tree Mortality, and Wildfire in Forests Adapted to Frequent Fire. *BioScience*.

Stephenson, N. L. 1998. "Actual evapotranspiration and deficit: Biologically meaningful correlates of vegetation distribution across spatial scales." J. Biogeog. 25:855–870.

Strauss, D., L. Bednar, and R. Mees. 1989. Do one percent of the forest fires cause ninety- nine percent of the damage? Forest Science 35:319-328.

Verdin, K.L. and Greenlee, S.K., 1996, January. Development of continental scale digital elevation models and extraction of hydrographic features. In Proceedings, third international conference/workshop on integrating GIS and environmental modeling, Santa Fe, New Mexico (pp. 21-26).

Voldoire, A., E. Sanchez-Gomez, D. Salas y Mélia, B. Decharme, C. Cassou, S.Sénési, S. Valcke, I. Beau, A. Alias, M. Chevallier, M. Déqué, J. Deshayes, H. Douville, E. Fernandez, G. Madec, E. Maisonnave , M.-P. Moine, S. Planton, D.Saint-Martin, S. Szopa, S. Tyteca, R. Alkama, S. Belamari, A. Braun, L. Coquart, F. Chauvin (2011) : The CNRM-CM5.1 global climate model: description and basic evaluation, Clim. Dyn., accepted, DOI:10.1007/s00382-011-1259-y.

Watanabe, M., Suzuki, T., O'ishi, R., Komuro, Y., Watanabe, S., Emori, S., Takemura, T., Chikira, M., Ogura, T., Sekiguchi, M. and Takata, K., 2010. Improved climate simulation by MIROC5: mean states, variability, and climate sensitivity. Journal of Climate, 23(23), pp.6312-6335.

Westerling, A.L., H.G. Hidalgo, D.R. Cayan, T.W. Swetnam 2006: "Warming and Earlier Spring Increases Western U.S. Forest Wildfire Activity" Science, 313: 940-943. DOI:10.1126/science.1128834.

Westerling, A. L. and B. P. Bryant, 2008: "Climate Change and Wildfire in California," Climatic Change, 87: s231-249. DOI:10.1007/s10584-007-9363-z.

Westerling, A. L. 2009: "Wildfires," Chapter 8 in Climate Change Science and Policy, Schneider, Mastrandrea, Rosencranz, Kuntz-Duriseti Eds., Island Press.

Westerling, A. L. , B. P. Bryant, H. K. Preisler, T.P. Holmes, H. G. Hidalgo, T. Das, S.R. Shrestha 2009: "Climate Change, Growth and California Wildfire" Public Interest Energy Research, California Energy Commision, Sacramento, CA.

Westerling, A.L., B.P. Bryant, H.K. Preisler, T.P. Holmes, H. Hidalgo, T. Das, and S. Shrestha 2011a: "Climate Change and Growth Scenarios for California Wildfire" Climatic Change, 109(s1):445-463.

Westerling, A.L., M.G. Turner, E.H. Smithwick, W.H. Romme, M.G. Ryan 2011b: "Continued warming could transform Greater Yellowstone fire regimes by mid-21st Century" Proceedings of the National Academy of Sciences, 108(32),13165-13170.

Westerling ALR. 2016 Increasing western US forest wildfire activity: sensitivity to changes in the timing of spring. Phil. Trans. R. Soc. B 371: 20150178. http://dx.doi.org/10.1098/rstb.2015.0178.

Zhang, Y.-H., M.J. Wooster, O. Tutubalina, and G.L.W. Perry. 2003. Monthly burned area and forest fire carbon emission estimates for the Russian Federation from SPOT VGT. Remote Sensing of Environment 87:1-15.

APPENDIX A: Supporting Figures

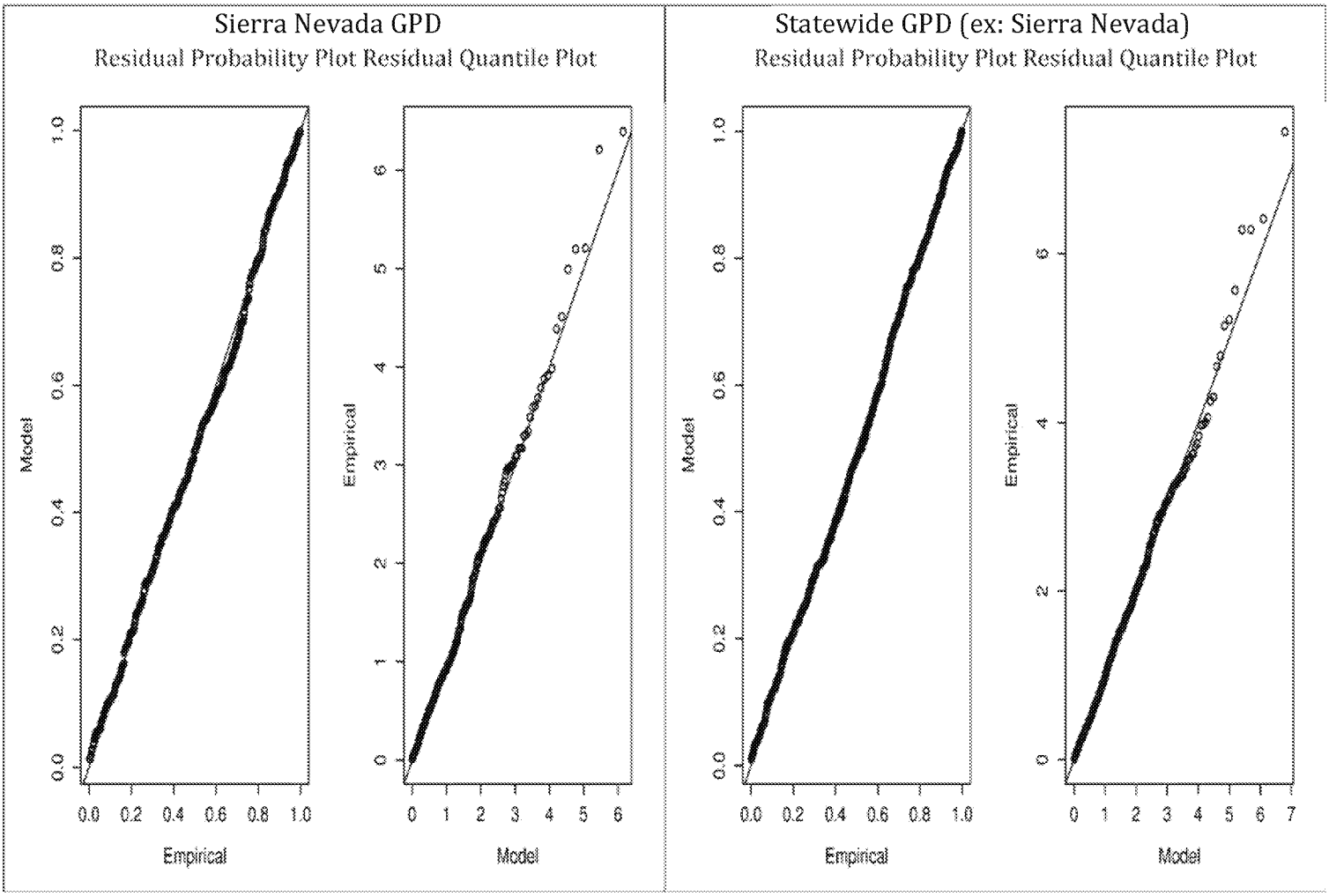

Figure A1: Residual Probability and residual quantile plots for Sierra Nevada (left) and Statewide, excluding Sierra Nevada (right).

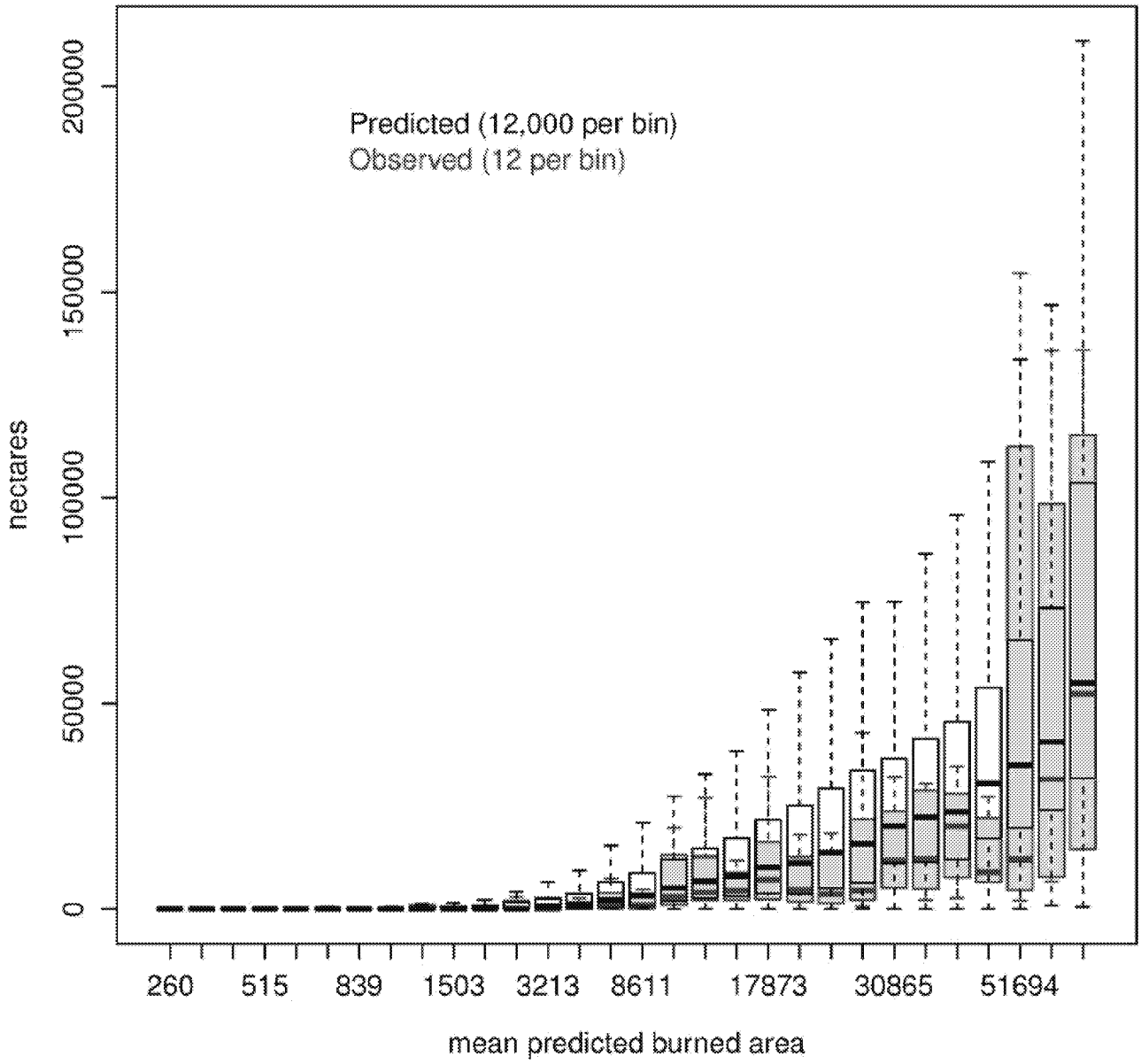

Figure A2: Binned monthly statewide predicted area burned in hectares (black boxplots) versus observed area burned (red boxplots). Monthly data for 30 years were aggregated statewide, ranked, and clustered in equal-sized bins corresponding to 12 ranked months. Sample size per observed bin is 12 observations of statewide area burned. For each predicted bin, 1000 simulations are included for each month, resulting in 12,000 member samples for each observed binned boxplot. Boxes show interquartile range, bold bars show medians, and whiskers denote 1.5 times the interquartile range.

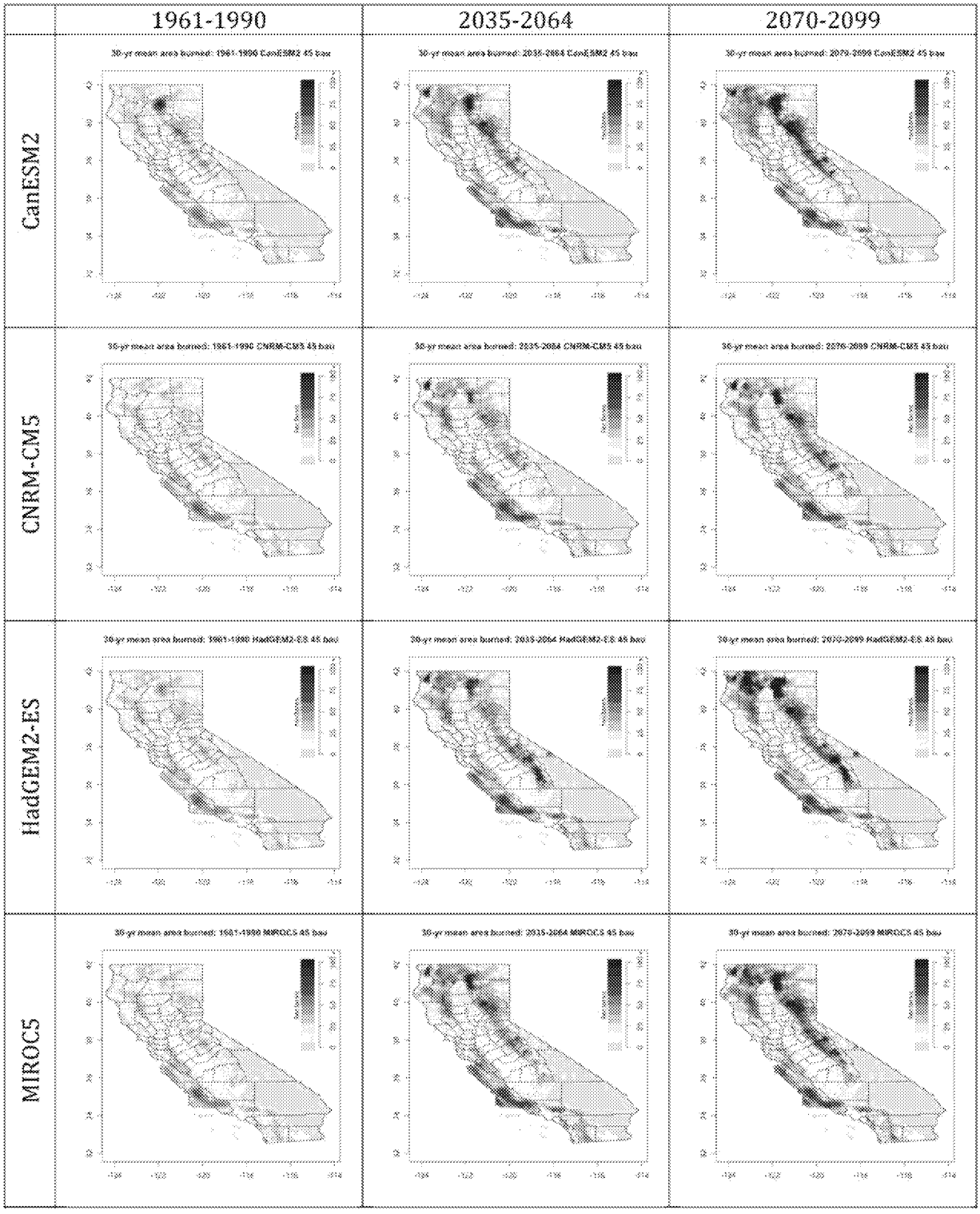

Figure A3: Average annual area burned by GCM and 30-year period for RCP 4.5, mid-range population growth.

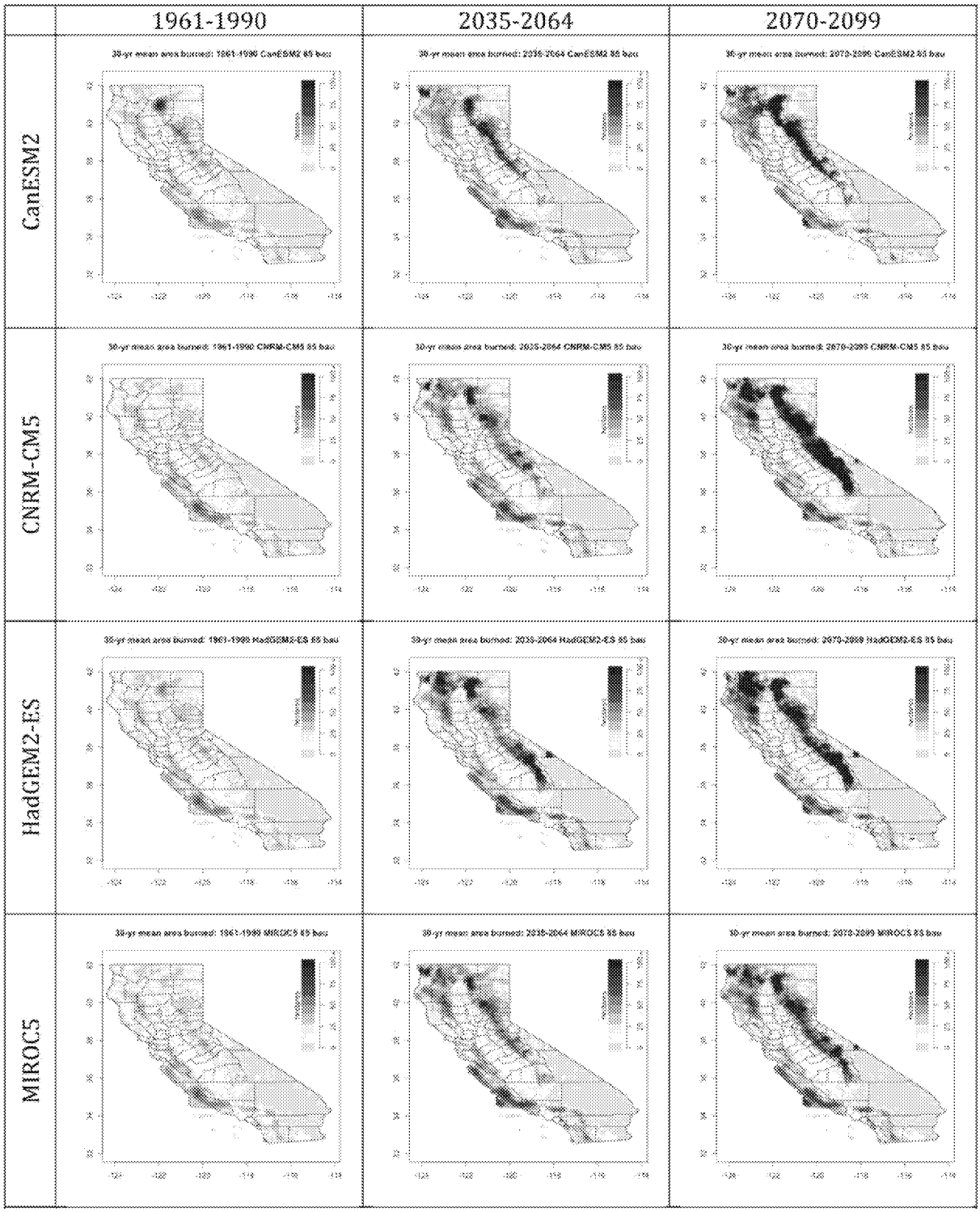

Figure A4: Average annual area burned by GCM and 30-year period for RCP 8.5, mid-range population growth.

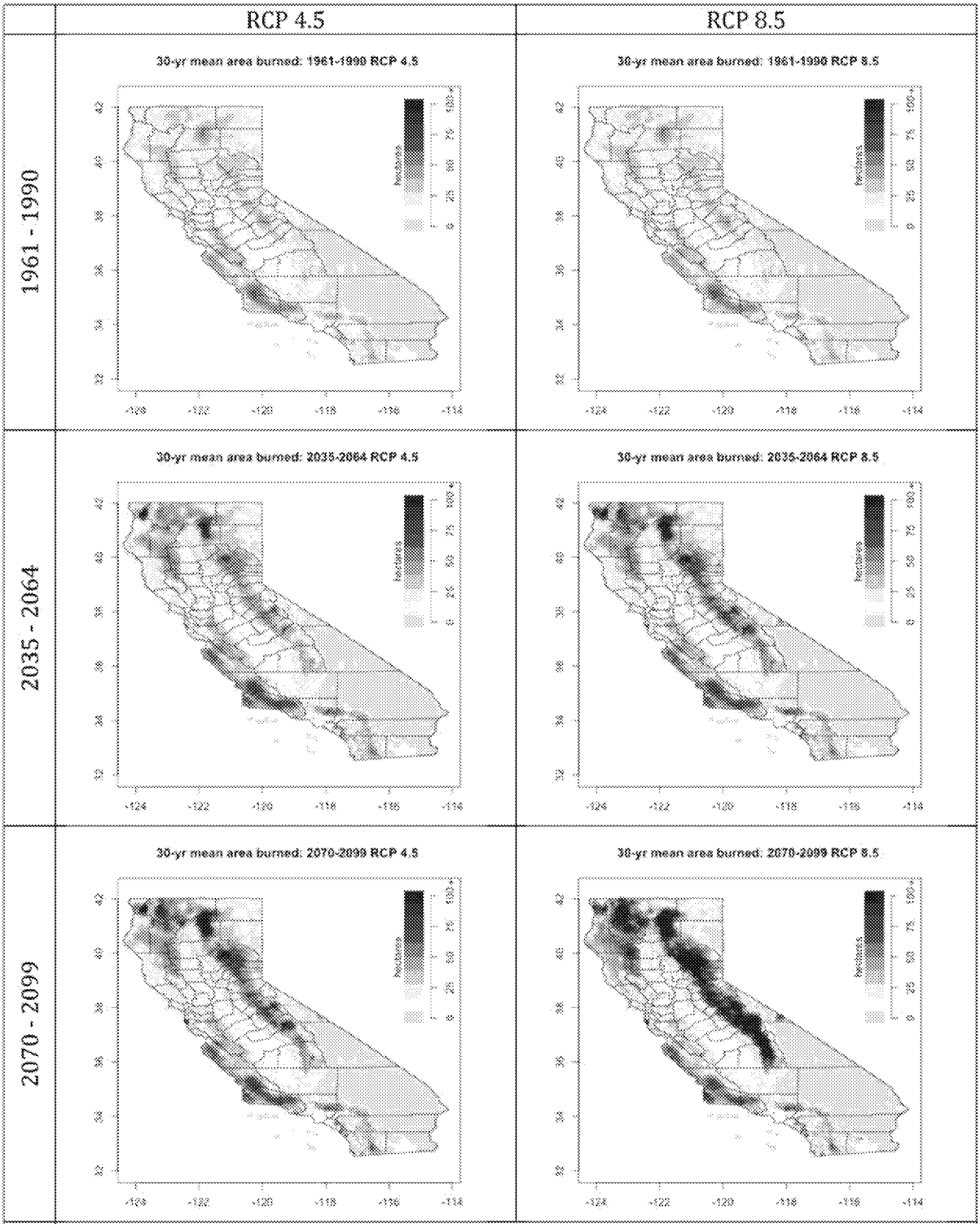

Figure A5: Average annual area burned composites: RCP 4.5 (left), RCP 8.5 (right), combining 4,320,000 simulations (30 years x 12 months x 1000 random draws x 4 GCMs x 3 population scenarios).

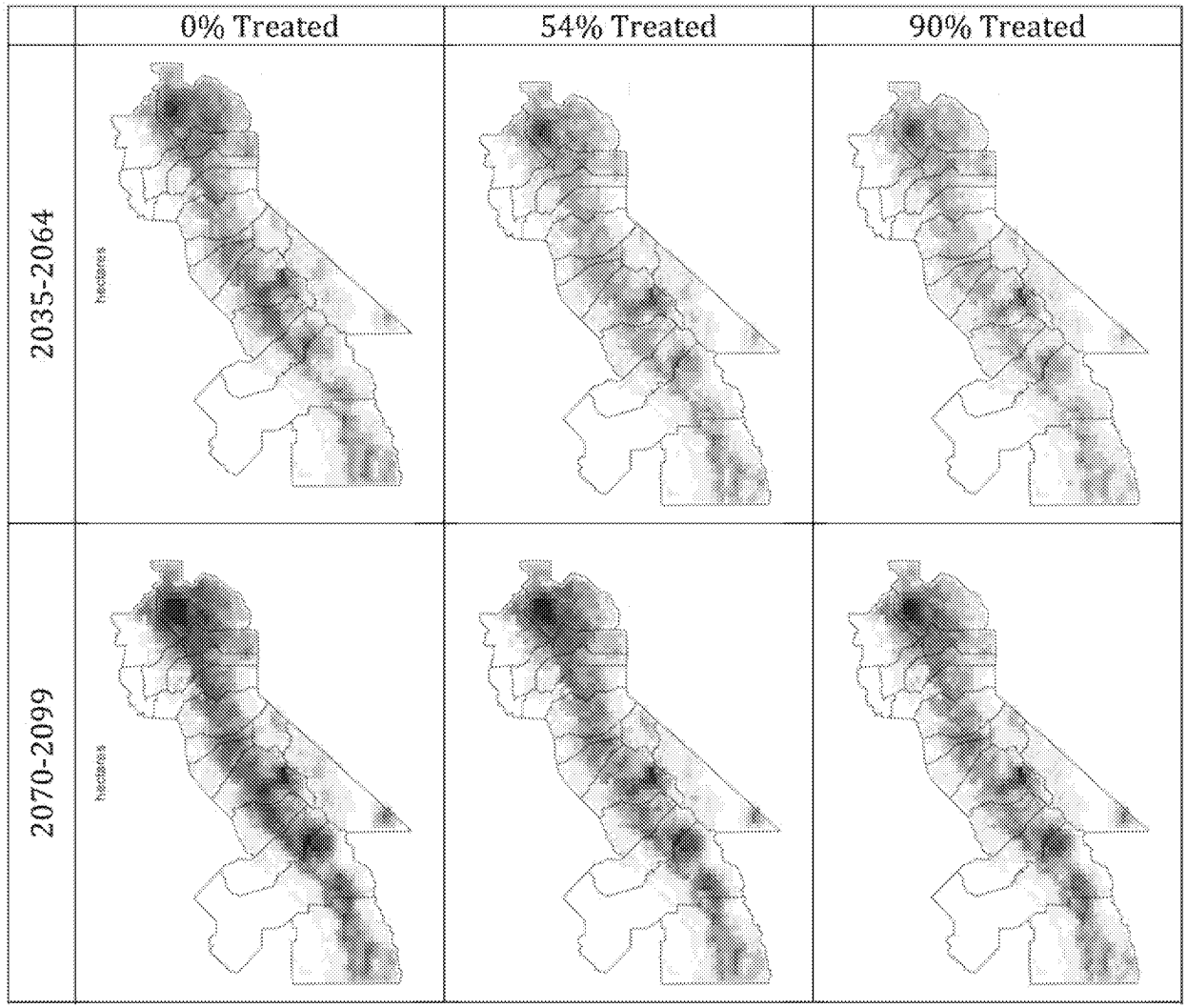

Figure A6: Average annual area burned composites for RCP 4.5: 0% (left), 54% (mid), and 90% (right) of altered forest fuels treated to restore pre/fire suppression fuel densities for mid/century (top) and end of century (bottom).

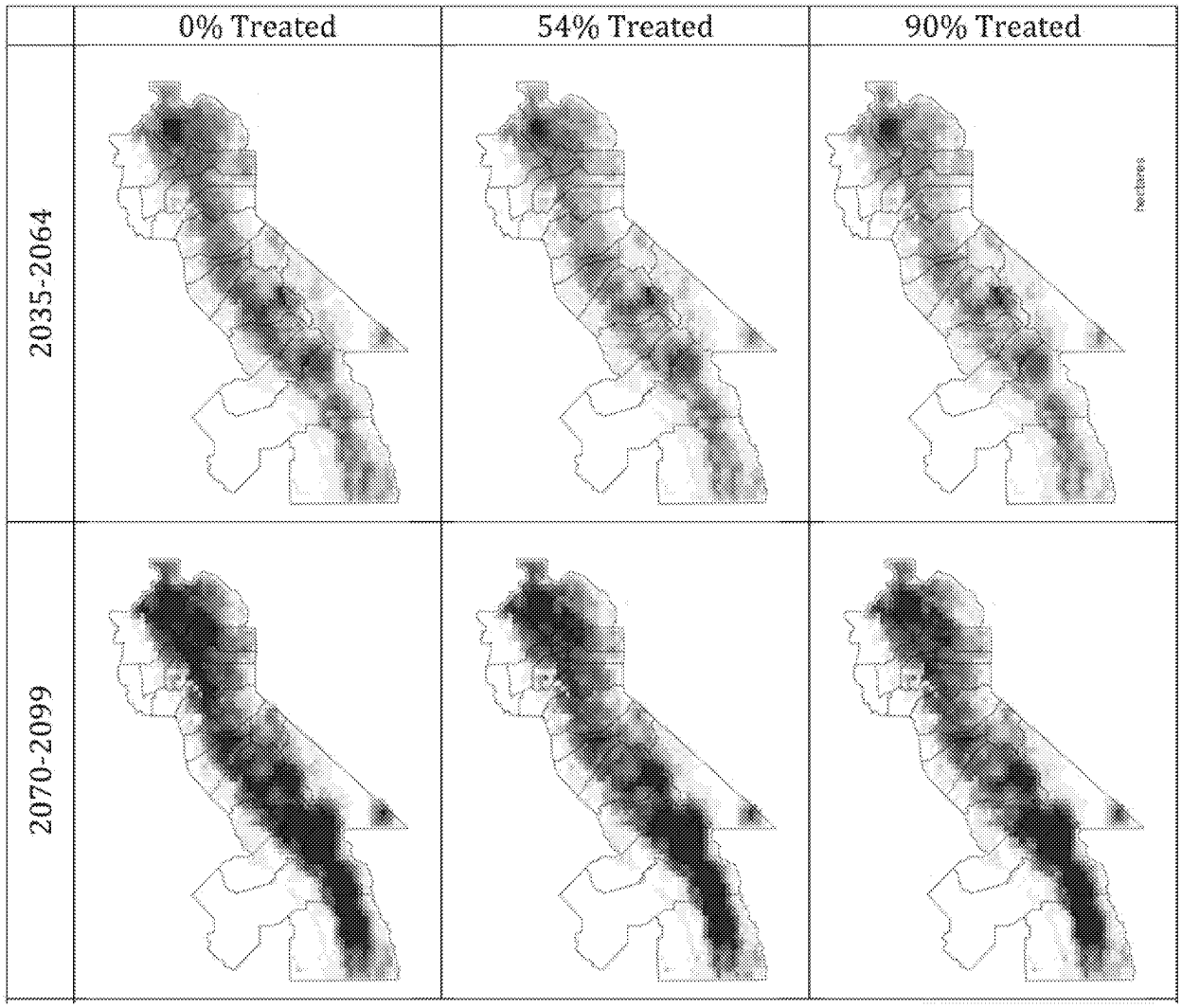

Figure A7: Average annual area burned composites for RCP 8.5: 0% (left), 54% (mid), and 90% (right) of altered forest fuels treated to restore pre/fire suppression fuel densities for mid/century (top) and end of century (bottom).

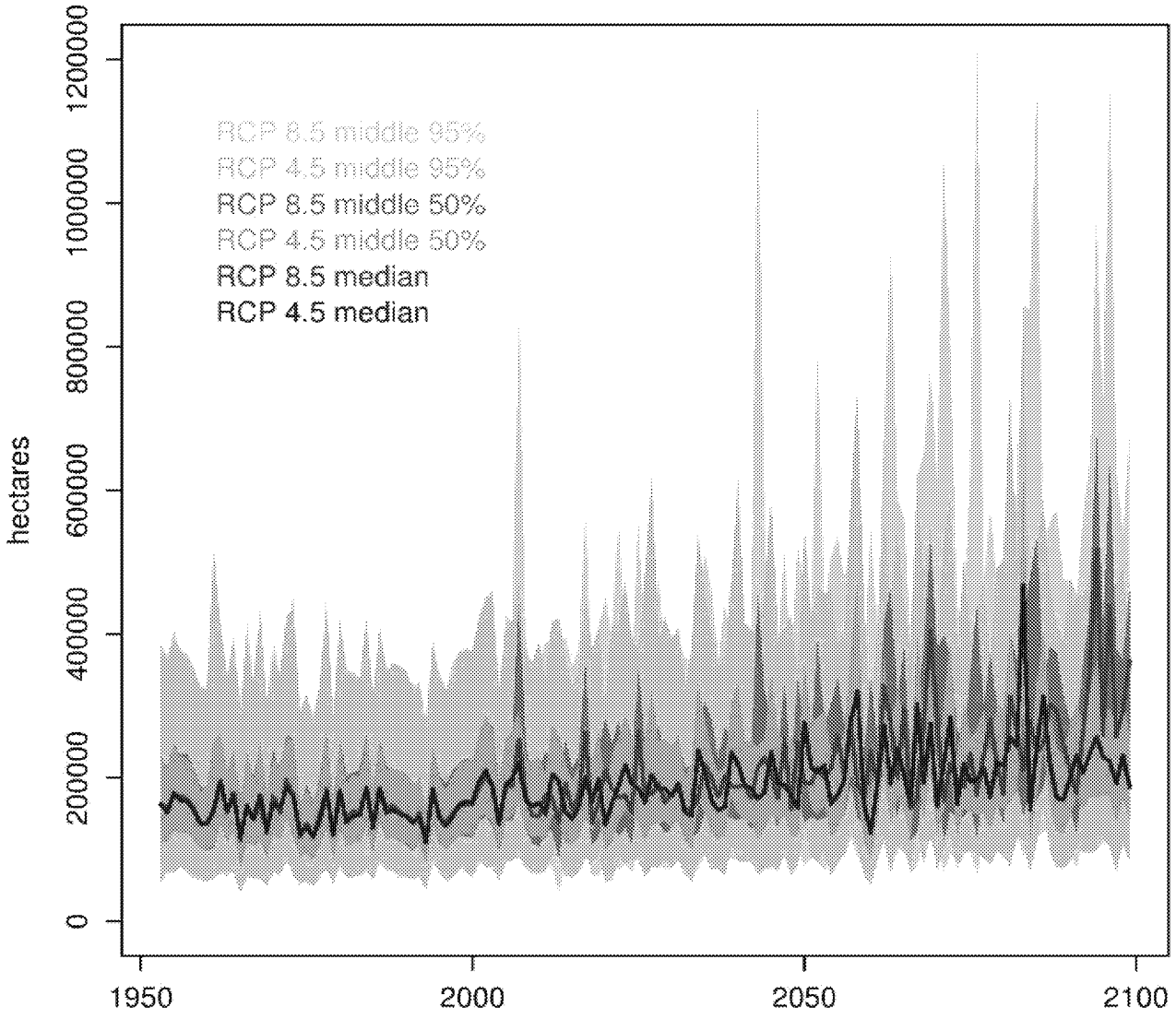

Figure A8: RCP4.5 vs 8.5 California Area Burned Quantities. Pooled simulations of annualized and aggregated statewide area burned for RCP 4.5 (blue) versus 8.5 (red). 100 randomly selected simulations from scenarios corresponding to each of four GCMs (CanESM2, CNRMKCM5, HadGEM2KES, MIROC5) and three population scenarios (low, mid and high range growth), resulting in 1200 simulations per year per RCP. Light shading shows middle 95%, dark shading shows middle 50%, and bold lines show median simulated values for statewide annual area burned.

APPENDIX B: Influence of Drought-related Tree Mortality on Wildfire Severity

B.1 Highlights

- Near-term impacts of tree-mortality on severely burned acreage via the effects of the desiccation and subsequent movement of fine fuels from the forest canopy to the surface are small (1% to 7%) relative to natural system variability.
- The impact of dead heavy fuels from tree mortality on wildfire after the first few decades, when heavy fuels have had time to cure and additional new biomass has developed, is without historical analogue for the scale of the recent dieback in the Sierra Nevada and cannot be quantified with empirical statistical models.

B.2 Introduction

An extreme multiyear drought centered on California beginning in the 2011-2012 water year and extending through 2015 was driven by an increased incidence of both temperature and precipitation extremes, and significantly associated with increases in wildfire area burned, high severity burned area, and drought-related tree mortality (Crockett and Westerling 2018). More than 100 million trees died (USDA 2016), with mortality significantly increasing with stand density and climatic water deficit (Young et al 2017). At fine spatial scales within the limited set of fires that intersect recent mortality data, patches of mortality were positively associated with subsequent fire, with hectares affected by fire 1.8 times larger on average in forest locations where roughly half the area was affected by tree mortality (Preisler et al 2017). Similarly, Stephens et al (2018) related stand level mortality up to between 40 and 60 percent to subsequent burned area in the Rough Fire.

Given these results, the question naturally arises: to what extent might widespread tree mortality in the Sierra Nevada affect subsequent high severity wildfire area burned? We focus in particular on high severity burned area, with the metric used here the area burned with ninety percent or more basal area killed (BA90), because of its ecological significance (e.g., in forest areas with 50% or more BA90, spotted owl nesting sites are abandoned (Jones et al 2016)), and the likelihood that very high severity burns are more liable to be a threat to infrastructure.

The challenge facing this kind of analysis is the paucity of observations of significant fires impinging on areas with widespread tree mortality at the scale and severity to be instructive regarding potential future fire risks after a singular event like this. Crockett and Westerling (2018) related fire area, fire severity and drought dieback to drought occurrence, but did not consider feedbacks from mortality into subsequent fire because of the limited data. Preisler et al (2017) worked at a finer spatial scale, considering the correlation between patches of vegetation affected by both morality and fire. Their limited data do not support an empirical test of the effect of mortality on the occurrence and size of high-severity fires. Stephens et al (2018) also worked at fine spatial scales, correlating stand level mortality with subsequent burn patches in

and around one fire. Numerous fires interacting with post-mortality forest fuels must be observed before a statistical model could be estimated.

Studies have been conducted examining the impact of tree mortality on subsequent wildfire severity in other ecosystems where widespread tree mortality has been occurring for longer, such as British Columbia and the northern U.S. Rockies (e.g., Hickes et al 2012, Harvey et al 2014). Because their fire regimes can be very different from that of the Sierra Nevada, with different characteristic fire severity and different climate-fire-vegetation interactions, these findings may not be relevant to assessing risks in Sierra Nevada forests and should only be used with caution.

Tree mortality count estimates are available from regular overflights for a limited set of years from the USFS Arial Detection Survey (https://www.fs.usda.gov/detail/r5/forest-grasslandhealth/?cid=fsbdev3_046677). These have been converted into estimated changes in live and dead biomass (Lara et al in press). However, the data for either estimating a statistical model relating high severity burned area to antecedent mortality or parameterizing and validating a dynamic model will remain sparse until sufficient time has passed to observe more fires impinging on the footprint of the recent widespread mortality event in the Sierra Nevada. In the absence of hard data, this analysis engages in scenario building. We apply expert opinion guided by the recent studies listed above (Stephens et al 2018, Preisler et al 2017), and allow for wide uncertainties, to consider what the potential near term effects might be of tree mortality on subsequent high severity wildfire.

B.3 Data Sources and Methods

Fire history data for large (>400 ha) wildfires were extracted from the Monitoring Trends in Burn Severity database (MTBS Data Access 2009, www.mtbs.gov; accessed 12/2008 and 9/2016), and coded by discovery date (month, year). We used ESRI Arc Macro Language (ESRI 1999) to intersect burn maps (at 30 m resolution) with a 1/16th degree grid, assigning each fire to the grid cell where a majority of the fire's area burned, or if multiple grid cells had similar areas burned, the one closest to the fire polygon centroid (Keyser and Westerling 2017). We then calculated area burned in patches within each fire where ninety percent or more of basal area was killed (BA90). Statistical wildfire models were then estimated using historical fire and climate data available for 1984–2014.

Estimates of Sierra Nevada live biomass in 2012 prior to the drought, and dead biomass post drought, were obtained from Tubbesing (UC Berkeley). Changes in dead biomass at 30 m resolution were calculated for Lara et al (in review) by combining Forest Service Aerial Detection Survey (ADS) data and the Landscape Ecology, Modeling, Mapping, and Analysis (LEMMA) team's Gradient Nearest Neighbor (GNN) Structure Maps (Ohmann JL, et al. (2012), Ohmann JL, et al. (2014), US Forest Service 2017, Wittwer 2008).

Additional vegetation characteristics data for the Sierra Nevada, in the form of fire regime condition class (FRCC) variables designed to measure the divergence of vegetation structure and composition from historical conditions (Hann et al 2008, Laverty and Williams 2000), were provided by the US Department of Agriculture's Forest Service Region 5 using the same methodology as the LANDFIRE project (Keane et al 2007, www.landfire.gov). FRCC classes 2 and 3 were combined (indicating ≥33% departure from historic conditions (Holsinger et al 2006, Keane et al 2007)) and aggregated to indicate fractional coverage of the 1/16th-degree lat/lon

(~6 km) grid used here. Fractional data were then normalized to provide a continuous variable not bounded by [0,1] as

$$\mathbf{FRCC23}_i = log((f23_i) / (1 - f23_i))$$

where $f23_i$ is the fractional vegetated area characterized as FRCC class 2 or 3 in grid cell i. Fuels management scenarios were constructed by randomly converting 30 m pixels within each federal land management unit from FRCC classes 2 and 3 to FRCC class 1 (ie., approximating historical conditions prior to the era fire suppression, with more open forest canopies, shorter fire rotations, and less severe fire (less biomass burned and less mature tree mortality)). Scenarios reported here examined converting, respectively, approximately 50% and 90% (R50 and R90 management scenarios) of the potentially treatable forest area to FRCC 1. Since the treatable area is far less than the total vegetated area, the treatments affect significantly less than 50% or 90% of the vegetated area. In practice, however, the treatments are large and at this scale would require substantial resources for a combination of mechanical tree removal and fires actively managed for fuels reduction objectives.

Gridded downscaled climate simulations for 1950-2099 from four global climate models using two emissions scenarios (RCP 4.5 and 8.5, see IPCC AR5 WG1, 2013) were obtained via Scripps Institution of Oceanography, including global models from Centre National de Recherches Météorologiques (CNRM-CM5, see Voldoire et al 2011), the Canadian Centre for Climate Modeling and Analysis (CanESM2, see Christian et al 2010, Arora and Boer 2010), the United Kingdom Met Office's Hadley Center (HadGEM2-ES, see Collins et al 2008), and the University of Tokyo's Center for Climate System Research (MIROC5, see Watanabe et al 2010).

B.4 Modeling Methods

Similar to the approach for total burned area, BA90 area was estimated using a generalized linear model for a threshold value (>50 ha) of BA90 being present conditional on a 400 ha fire being present and on climate. The conditional extent of BA90 area was estimated using a generalized Pareto distribution fit to climate and vegetation characteristics as covariates. Model specifications were assessed using the Akaike Information Criterion (Akaike 1974). The same suite of potential independent variables was considered, with the addition of dead biomass.

A set of scenarios were constructed to illustrate possible influences of tree mortality on BA90 area. Examination of the large fire record revealed that no large fires with significant BA90 area occurred in the record after the first year of the drought, leaving an insufficient sample to statistically calculate the effects of mortality on subsequent BA90 area at the spatial scale used here (a 1/16 degree grid). Expert opinion on potential risks was solicited from USDA Forest Service Region 5 management and affiliated researchers. The result was a set of heuristics recommended by USFS Region 5 staff as follows:

- years 0-3: in grid cells with 50% or more mortality, increase the risk of high severity fire by 20, 50 and 70 percent, reflecting broad uncertainty about potential impacts. In grid cells with less than 50% mortality, assume the pre-drought risk holds, due to the extreme uncertainty.

- years 4-15: in grid cells with 50% or more mortality, decrease the risk of high severity fire by 25%, reflecting the loss of fine canopy fuels.

These rules are meant to cover the evolution of tree mortality influences on the risk of high severity (here BA90) wildfire. First, that at the time of and shortly after a mortality event, fine canopy fuels are still present in the canopy and become increasingly desiccated (0-3 years post mortality). After a short time, however, these fine fuels (needles) fall from the canopy, reducing the risk of canopy fires that can produce high severity burns, but also increasing fine surface fuels for a time (4-15 years post mortality). (See Stephens et al 2018 for a more detailed discussion).

The probability of high severity fire conditional on a large fire occurring is historically high (calculated here as greater than 50% on average), no increase in the occurrence of the threshold BA90 area (>50 ha) was observed during the drought, and >50 ha is also a low threshold for BA90 presence, so the probability of the presence/absence of >50 ha of BA90 was not adjusted in building the scenarios. The effect of mortality was only modeled by adjusting the scale parameter for the BA90 GPD. The scale parameter for the generalized Pareto distribution fit to historic BA90 area was adjusted according to the heuristics described above to yield scenarios for a wide range of hypothesized changes in high severity burned area in response to widespread tree mortality.

For each of the 106 grid points with 50% or greater mortality observed, comparisons were made pairing BA90 simulations for post-mortality fire risk scenarios (20%, 50% and 70% increased GPD scale parameters) with BA90 simulations for the baseline risk scenario for 0 - 3 and 4 - 15 years post drought in t.tests.

B.5 Results

The best fit presence/absence model for 50 ha or more of BA90 area was a generalized linear model using cumulative monthly climate water deficit ($\boldsymbol{CWD}_{ij}$), cumulative monthly actual evapotranspiration ($\boldsymbol{AET}_{ij}$), cumulative water year climate water deficit ($\boldsymbol{CWD0}_{ij}$), and JJA average temperature ($\boldsymbol{Tjja}_{ij}$). The best fit generalized Pareto distribution for BA90 extent was a function of $\boldsymbol{CWD}_{ij}$, $\boldsymbol{CWD0}_{ij}$, MAM average temperature ($\boldsymbol{Tmam}_{ij}$), the fraction of grid cell vegetated area classified in FRCC 2 and 3 ($\boldsymbol{FRCC23}_{ij}$), and a snapshot of live biomass per grid cell in 2012 ($\boldsymbol{BM2012}_{ij}$) (Figure B1). The generalized Pareto model fit to these data closely tracks the largest observed BA90 area quantiles, which are often difficult to model due to differences in the processes that govern average versus extreme high severity fire extents (Figure B1).

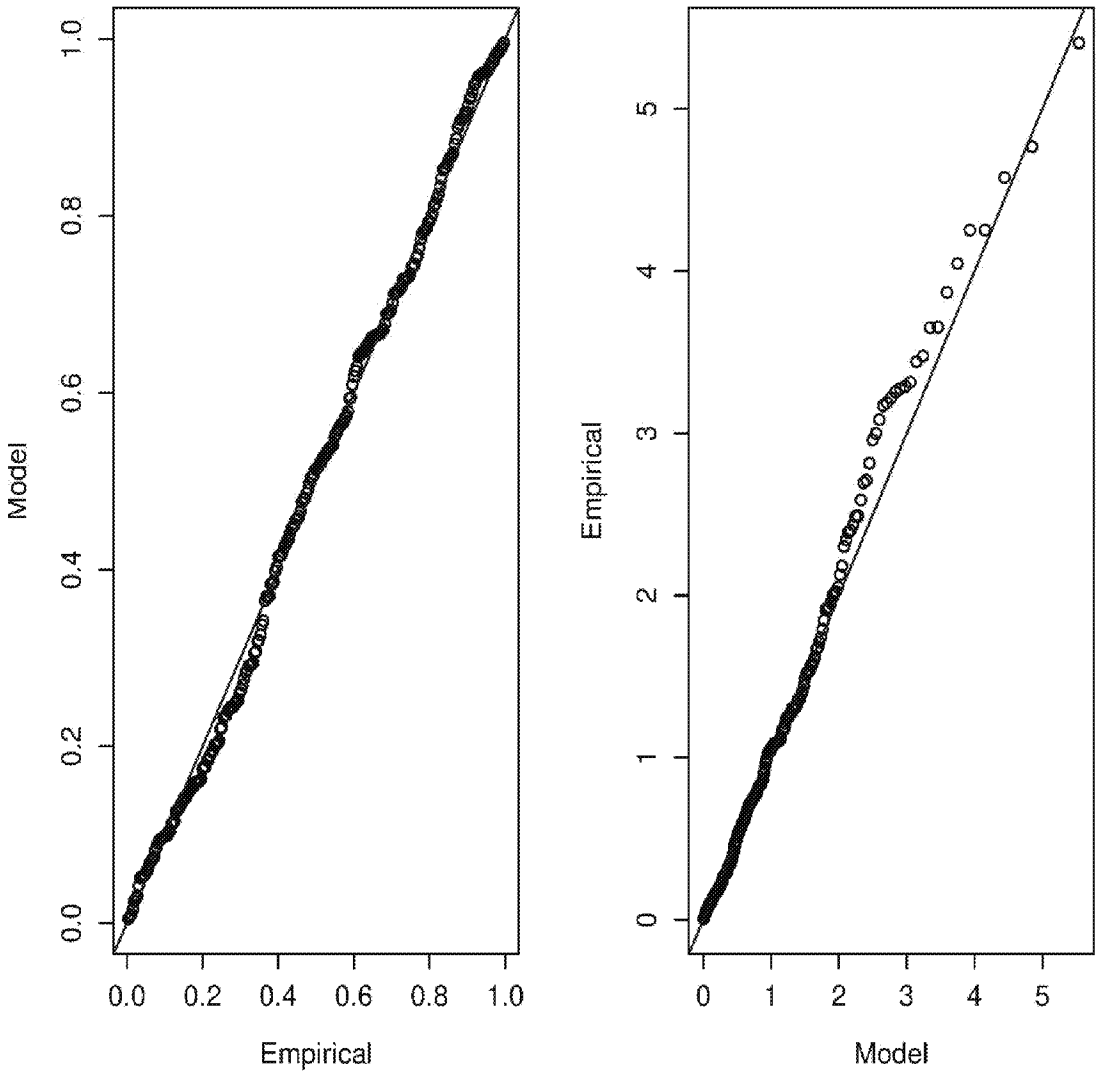

Figure B1: Generalized Pareto fit to BA90 burned area and covariates: residual probability plot (left) and residual quantile plot (right).

While the changes to fire risk imposed by the heuristics were substantial, they only applied in grid cells (*j*) where 50% or more dead biomass was observed, while the natural variability in high BA90 area is large. Consequently, the fractional change in BA90 area attributed to biomass effects here is relatively small and insignificant when considered from the perspective of the Sierra Nevada region as a whole: ranging from a less than 7% increase for the 70% scenario to less than 1% for the 20% scenario, averaged over all four global climate models. Most of the effect is concentrated where the highest mortality occurred, along the western slopes of the central and southern Sierra Nevada (Figure B2 - B6). However, significant t-tests for grid cells in these areas were no more numerous than what would be expected to be observed by chance. In other words, the effects on BA90 postulated for each scenario were small compared to the

background variability inherent in the modeled system. This is not surprising, given the extreme fat tail distributions that characterize both fire size and high severity burned area.

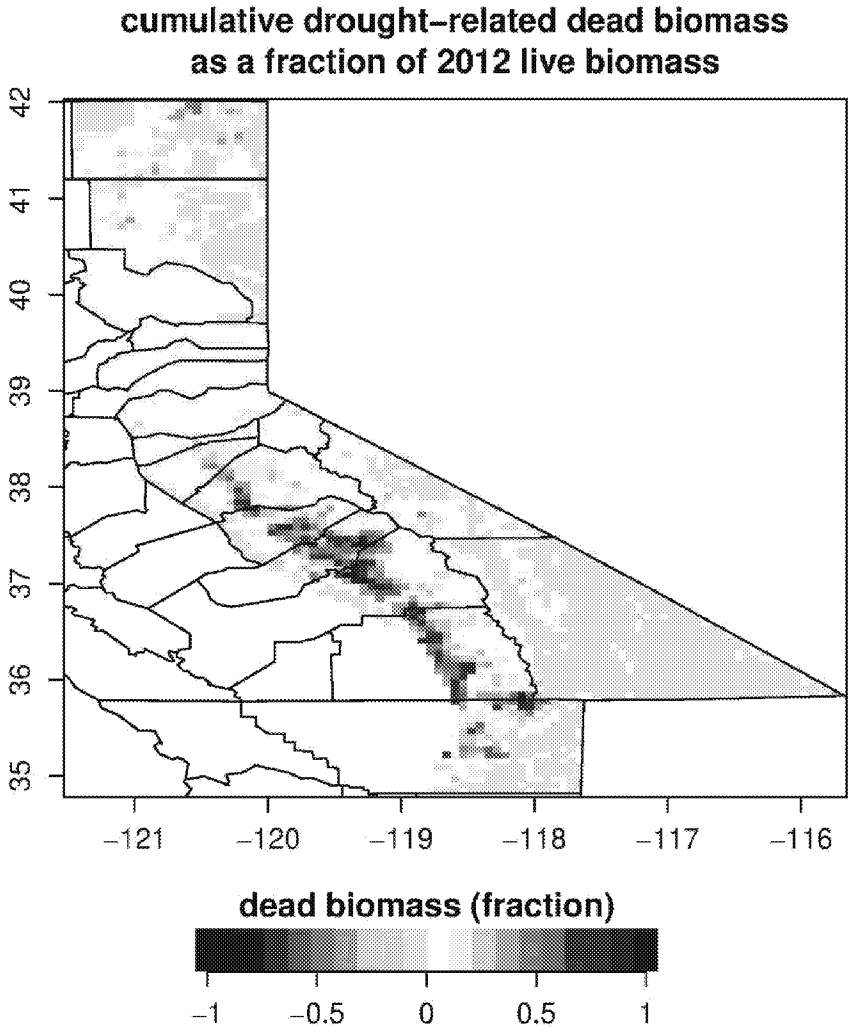

Figure B2. Cumulative drought-related dead biomass as a fraction of estimated 2012 live biomass (Lara et al 2018).

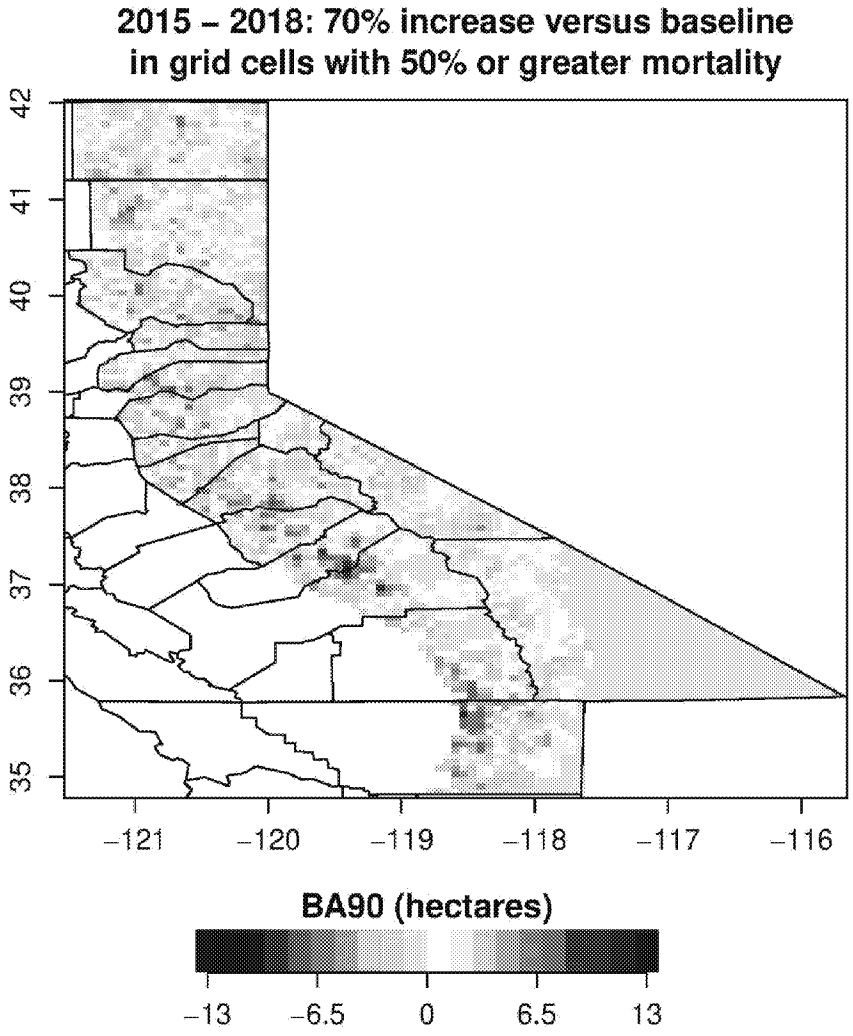

Figure B3. BA90 scenario: Average annual change in BA90 simulated with an assumed 70% increase in the generalized Pareto distribution scale parameter for years 0-3 post-drought.

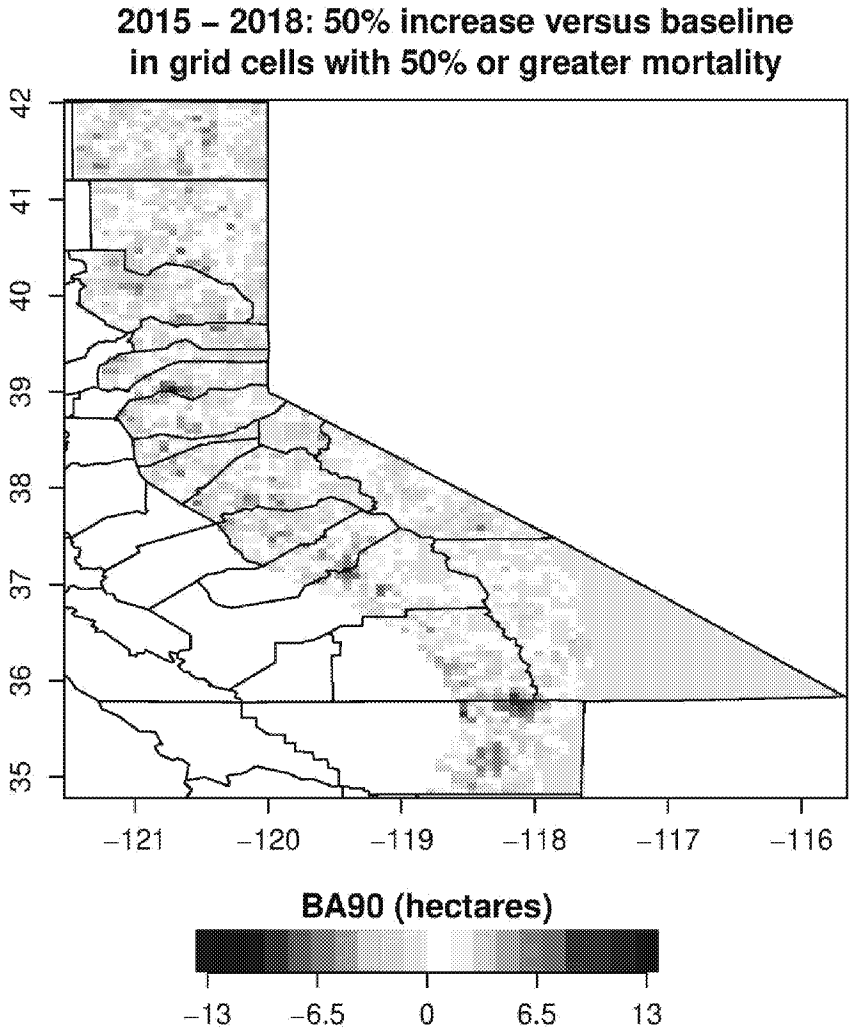

Figure B4. BA90 scenario: Average annual change in BA90 simulated with an assumed 50% increase in the generalized Pareto distribution scale parameter for years 0-3 post-drought.

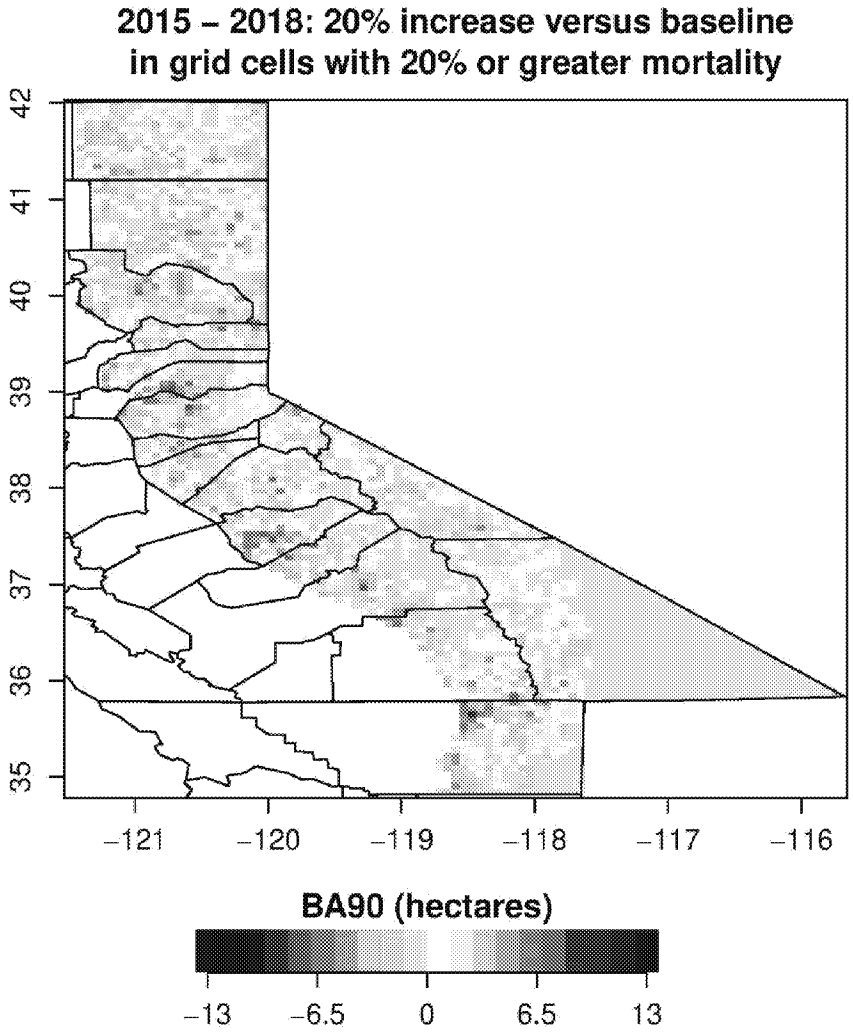

Figure B5. BA90 scenario: Average annual change in BA90 simulated with an assumed 20% increase in the generalized Pareto distribution scale parameter for years 0-3 post-drought.

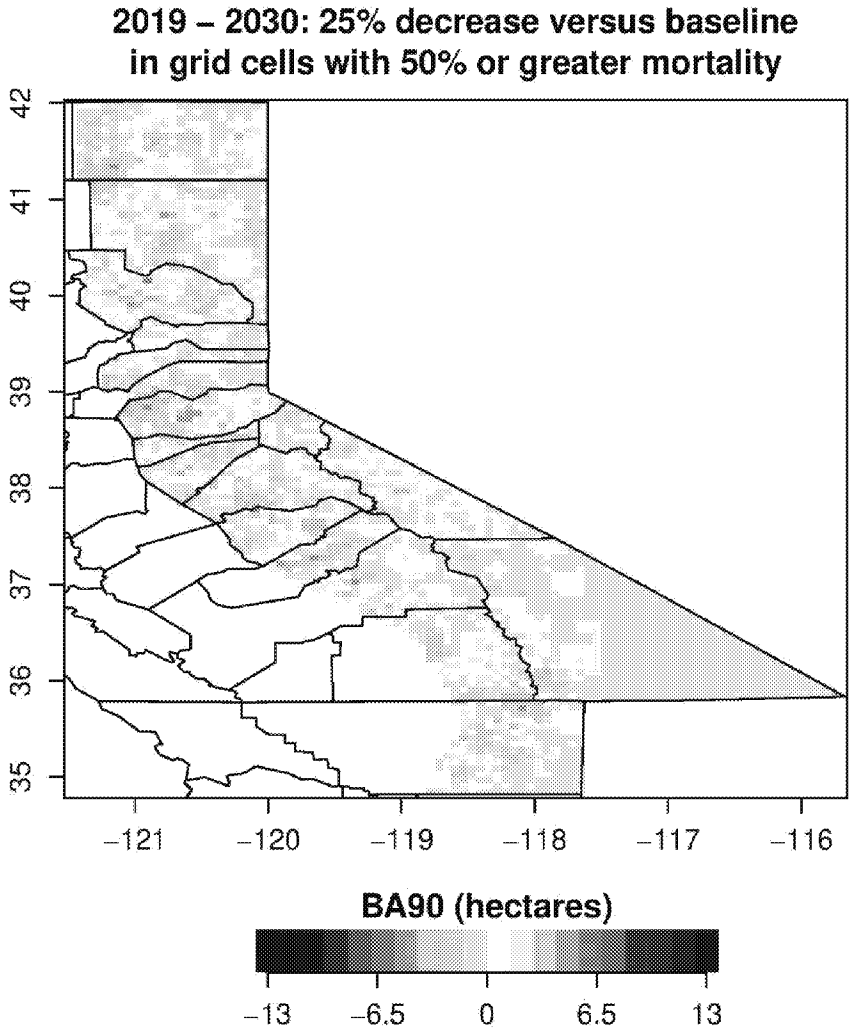

Figure B6. BA90 scenario: Average annual change in BA90 simulated with an assumed 25% decrease in the generalized Pareto distribution scale parameter for years 4-15 post-drought.

B.6 Discussion

The analysis described here gives a preliminary look at postulated near term effects of tree mortality on BA90 burned area. These were small compared to inherent variability in the system, even when assuming very large shifts in the BA90 size distribution. This is primarily because the area with 50% or more mortality is concentrated over a relatively small portion of the Sierra Nevada. And for forest with less than 50% mortality, there was no basis to support a change in the fire size distribution. However, our modeling focused only on the effects of the desiccation and movement of fine canopy fuels to the surface fuel layer. An additional

postulated potential effect further into the future is that there might exist a risk of mass fires once a substantial quantity of dead and down heavy fuels (logs) cure out and sufficient fine fuels grow up around them to facilitate the spread of a fire severe enough to ignite these fuels (see for example Stephens et al 2018). There are no recent historical analogs for this situation that would provide data for this ecosystem. Analogues might be mass fires in German and Japanese cities firebombed in World War II, or perhaps the cumulated slash from clear cutting in US Rocky Mountain forests prior to the fires of 1910. Given the paucity of data, current models have as yet no basis for quantifying the risk of mass fire in the Sierra Nevada mid-century or beyond.

B.7 Acknowledgements

Many thanks to Zachary Heath Region 5 Forest Health Protection for the ADS data, to Carmen Tubbesing for sharing estimated live and dead biomass data, Haiganoush Preisler for gridded ADS data and advice, and Brandon Collins and Sarah Sawyer for suggesting heuristics for modifying fire risk scenarios.

B.8 References

Akaike H. 1974. A new look at the statistical model identification. IEEE Trans Automatic Control. 19(6): 716-723.

Christian, J.R., Arora, V.K., Boer, G.J., Curry, C.L., Zahariev, K., Denman, K.L., Flato, G.M., Lee, W.G., Merryfield, W.J., Roulet, N.T. and Scinocca, J.F., 2010. The global carbon cycle in the Canadian Earth system model (CanESM1): Preindustrial control simulation. *Journal of Geophysical Research: Biogeosciences*, *115*(G3).

Collins, W.J., N. Bellouin, M. Doutriaux-Boucher, N. Gedney, T. Hinton, C. D. Jones, S. Liddicoat, G. Martin, F. O'Connor, J. Rae, C. Senior, I. Totterdell, S. Woodward, T. Reichler, J. Kim, 2008: Evaluation of the HadGEM2 model. Met Office Hadley Centre Technical Note no. HCTN 74, available from Met Office, FitzRoy Road, Exeter EX1 3PB http://www.metoffice.gov.uk/publications/HCTN/index.html

Crockett, J.L. and Westerling, A.L., 2018. Greater temperature and precipitation extremes intensify Western US droughts, wildfire severity, and Sierra Nevada tree mortality. Journal of Climate, 31(1), pp.341-354.

ESRI 1999 Arc Macro Language version 7.1.1: Developing ARC/INFO Menus and Macros with AML, for UNIX and Windows NT 2nd edn (Redlands, CA: ESRI Press) editors

Hann, W., Shlisky, A., Havlina, D., Schon, K., Barrett, S., DeMeo, T., Pohl, K., Menakis, J., Hamilton, D., Jones, J. and Levesque, M., 2004. Interagency fire regime condition class guidebook. National Interagency Fire Center: Boise, ID) Available at http://www. frcc. gov/[Verified April 2008].

Harvey, B.J., Donato, D.C. and Turner, M.G., 2014. Recent mountain pine beetle outbreaks, wildfire severity, and postfire tree regeneration in the US Northern Rockies. Proceedings of the National Academy of Sciences, 111(42), pp.15120-15125.

Hicke, J.A., Johnson, M.C., Hayes, J.L. and Preisler, H.K., 2012. Effects of bark beetle-caused tree mortality on wildfire. Forest Ecology and Management, 271, pp.81-90.

Holsinger, Lisa, Keane, R.E., Parsons, R., Karau, E., 2006. Development of biophysical gradient layers for the LANDFIRE prototype project. In: Rollins, M.G., Frame, C. (Eds.), The, LANDFIRE, Prototype Project: Nationally Consistent, Locally Relevant Geospatial Data for Wildland Fire, Management, USDA, Forest Service Rocky Mountain Research Station General Technical Report, RMRS-GTR-175.

IPCC AR5 WG1 (2013), Stocker, T.F.; et al., eds., Climate Change 2013: The Physical Science Basis. Working Group 1 (WG1) Contribution to the Intergovernmental Panel on Climate Change (IPCC) 5th Assessment Report (AR5), Cambridge University Press.

Johnson E, Wittwer D (2008) Aerial detection surveys in the united states. Australian Forestry 71(3):212–215.

Jones, G.M., Gutiérrez, R.J., Tempel, D.J., Whitmore, S.A., Berigan, W.J. and Peery, M.Z., 2016. Megafires: an emerging threat to old-forest species. Frontiers in Ecology and the Environment, 14(6), pp.300-306.

Keane, R.E., Rollins, M. and Zhu, Z.L., 2007. Using simulated historical time series to prioritize fuel treatments on landscapes across the United States: the LANDFIRE prototype project. ecological modelling, 204(3-4), pp.485-502.

Keyser, A.R. & Westerling, A.L. 2017. Climate drives inter-annual variability in probability of high severity fire occurrence in the western United States. Environmental Research Letters. 12: 065003.

Laverty, L., Williams, J., 2000. Protecting people and sustaining resources in fire-adapted ecosystems—a cohesive strategy. Forest Service response to GAO Report GAO/RCED 99-65. USDA Forest Service, Washington, DC.

Ohmann JL, et al. (2012) Mapping change of older forest with nearest-neighbor imputation and landsat time-series. Forest Ecology and Management 272:13–25.

Ohmann JL, Gregory MJ, Roberts HM (2014) Scale considerations for integrating forest inventory plot data and satellite image data for regional forest mapping. Remote sensing of environment 151:3–15.

Preisler, H.K., Grulke, N.E., Heath, Z. and Smith, S.L., 2017. Analysis and out-year forecast of beetle, borer, and drought-induced tree mortality in California. Forest Ecology and Management, 399, pp.166-178.

Stephens, Scott L; Collins, Brandon M; Fettig, Christopher J; Finney, Mark A; Hoffman, Chad M; Knapp, Eric E; North, Malcolm P; Safford, Hugh; Wayman, Rebecca B 2018. Drought, Tree Mortality, and Wildfire in Forests Adapted to Frequent Fire. BioScience. 68(2): 77-88. https://doi.org/10.1093/biosci/bix146.

U.S. Forest Service (2017) U.s. forest service pacific southwest region forest health protection aerial detection survey. Available at: https://www.fs.usda.gov/detail/r5/forest-grasslandhealth/?cid=fsbdev3_046696/ [Accessed March 14, 2017].

USDA 2016. News Release No. 0246.16 New Aerial Survey Identifies More Than 100 Million Dead Trees in California https://www.usda.gov/media/press-releases/2016/11/18/new-aerial-survey-identifies-more-100-million-dead-trees-california

Voldoire, A., E. Sanchez-Gomez, D. Salas y Mélia, B. Decharme, C. Cassou, S.Sénési, S. Valcke, I. Beau, A. Alias, M. Chevallier, M. Déqué, J. Deshayes, H. Douville, E. Fernandez, G. Madec, E. Maisonnave , M.-P. Moine, S. Planton, D.Saint-Martin, S. Szopa, S. Tyteca, R. Alkama, S. Belamari, A. Braun, L. Coquart, F. Chauvin (2011) : The CNRM-CM5.1 global climate model: description and basic evaluation, Clim. Dyn., accepted, DOI:10.1007/s00382-011-1259-y.

Watanabe, M., Suzuki, T., O'ishi, R., Komuro, Y., Watanabe, S., Emori, S., Takemura, T., Chikira, M., Ogura, T., Sekiguchi, M. and Takata, K., 2010. Improved climate simulation by MIROC5: mean states, variability, and climate sensitivity. Journal of Climate, 23(23), pp.6312-6335.

Young, D.J., Stevens, J.T., Earles, J.M., Moore, J., Ellis, A., Jirka, A.L. and Latimer, A.M., 2017. Long-term climate and competition explain forest mortality patterns under extreme drought. Ecology letters, 20(1), pp.78-86.